Title

An assessment of the load modifying potential of model predictive controlled dynamic facades within the California context

Authors

Gehbauer, C
Blum, DH
Wang, T
et al.

Publication Date

2020-03-01

DOI

10.1016/j.enbuild.2020.109762

Peer reviewed

DOI 10.1016/j.enbuild.2020.109762

Lawrence Berkeley National Laboratory

An assessment of the load modifying potential of model predictive controlled dynamic facades within the California context

Christoph Gehbauer, David H. Blum, Taoning Wang, Eleanor S. Lee

Lawrence Berkeley National Laboratory

Energy Technologies Area

January 2020

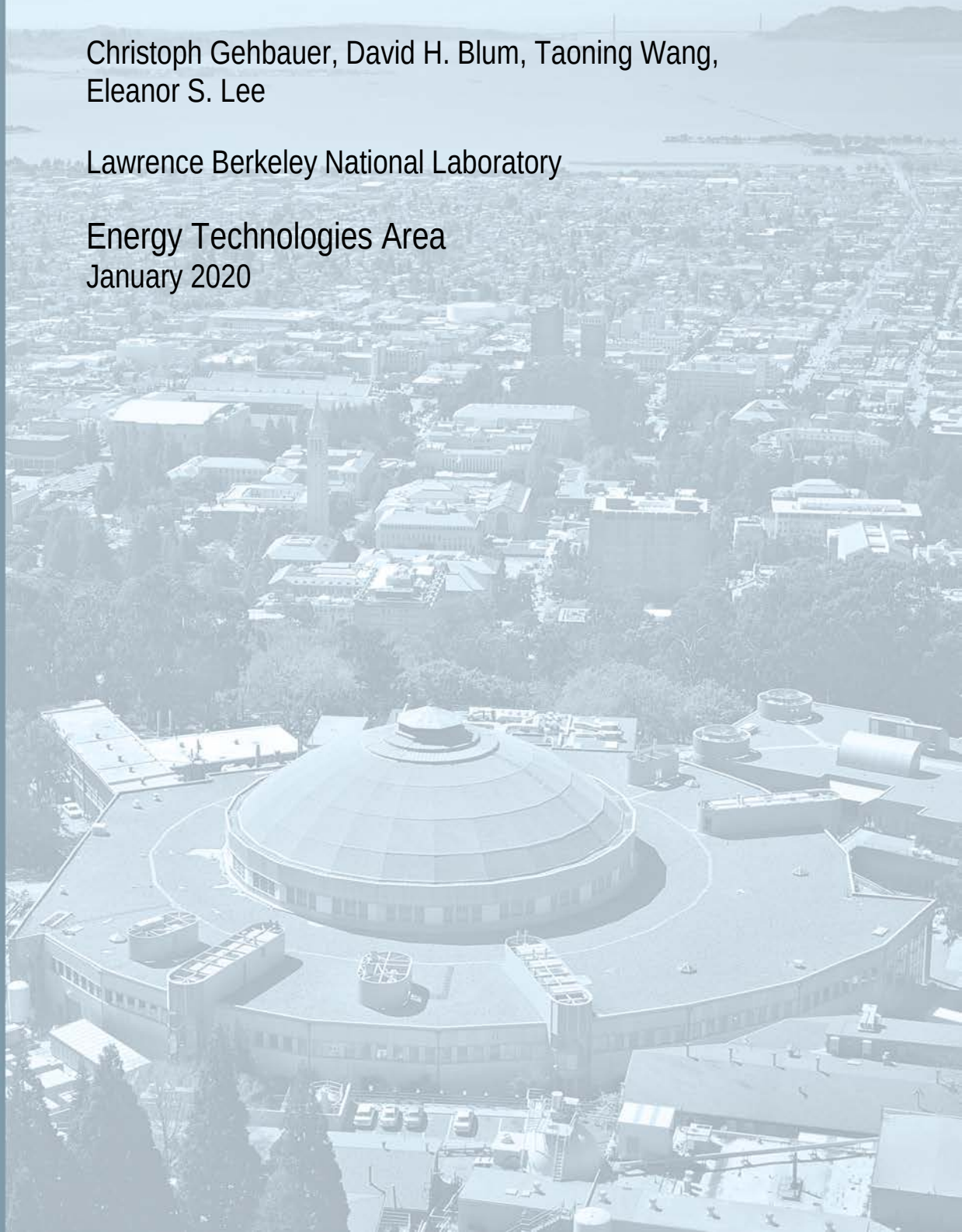

Disclaimer:

Acknowledgments:

This work was supported by the California Energy Commission through its Electric Program Investment Charge (EPIC) Program on behalf of the citizens of California and the Assistant Secretary for Energy Efficiency and Renewable Energy, Building Technologies Program, of the U.S. Department of Energy, under Contract No. DE-AC02-05CH11231.

The authors would like to thank Dustin Davis at the California Energy Commission and Marc LaFrance and Amir Roth at the U.S. Department of Energy for their continued support for this research. We would like to also acknowledge our LBNL colleagues Thierry Nouidui and Daniel Fuller for their technical support for this research.

An assessment of the load modifying potential of model predictive controlled dynamic facades within the California context

Christoph Gehbauer*, David H. Blum, Taoning Wang, Eleanor S. Lee

Building Technology and Urban Systems Division, Energy Technologies Area,
Lawrence Berkeley National Laboratory, Mailstop 90-3147,
1 Cyclotron Road, Berkeley, California 94720 USA

Abstract

California is making major strides towards meeting its greenhouse gas emission reduction goals with the transformation of its electrical grid to accommodate renewable generation, aggressive promotion of building energy efficiency, and increased emphasis on moving toward electrification of end uses (e.g., residential heating, etc.). As a result of this activity, the State is faced with significant challenges of system wide resource adequacy, power quality and grid reliability that could be addressed in part with demand responsive (DR) load modifying strategies using controllable building technologies. Dynamic facades have the ability to potentially shift and shed loads at critical times of the day in combination with daylighting and HVAC controls. This study explores the technical potential of dynamic facades to support net load shape objectives. A model predictive controller (MPC) was designed based on reduced order thermal (Modelica) and window (Radiance) models. Using an automated workflow (involving JModelica.org and MPCPy), these models were converted and differentiated to formulate a non-linear optimization problem. A gradient-based, non-linear programming problem solver (IPOPT) was used to derive an optimal control strategy, then a post-optimization step was used to convert the solution to a discrete state for facade actuation. Continuous state modulation of the façade was also modeled. The performance of the MPC controller with and without activation of thermal mass was evaluated in a south-facing perimeter office zone with a three-zone electrochromic window for a clear sunny week during summer and winter periods in Oakland and Burbank, California. MPC strategies reduced total energy cost by 9-28% and critical coincident peak demand was reduced by up to 0.58 W/ft^2-floor or 19-43% in the 4.6 m (15 ft) deep south zone on sunny summer days in Oakland compared to state-of-the-art heuristic control. Similar savings were achieved for the hotter, Burbank climate in Southern California. This outcome supports the argument that MPC control of dynamic facades can provide significant electricity cost reductions and net load management capabilities of benefit to both the building owner and evolving electrical grid.

Keywords: model predictive controls; switchable windows; dynamic facades; daylighting; windows; building energy efficiency; controller in the loop.

* Corresponding author, cgehbauer@lbl.gov (C. Gehbauer)

1. Introduction

California's electricity system has been transformed over the past decade with renewable generation accounting for 27% of the electricity supply in 2016 towards a goal of 50% by 2030. Per capita energy use has remained nearly level between 1993 and 2005 [CEC 2017]. Despite these impressive achievements, significant progress is still needed to meet California's requirements for greenhouse gas (GHG) emission reductions of 40% below 1990 levels by 2030 and 80% below 1990 levels by 2050. In a study forecasting total California electricity demand, the authors concluded that transformational solutions are needed to achieve California's 2050 GHG reduction goal [Wei et al. 2013a]. The study identified a portfolio of measures, where increased efficiency in the buildings, transportation and industry sectors represented 43% of the requisite GHG reduction, with the remaining reductions coming from low-GHG sources of electricity (e.g., renewable energy, carbon capture, nuclear), a switch from natural gas to electricity as a source for heating, electric vehicles, biofuels, and conservation measures. Assuming electrification of heating energy will be needed to meet GHG goals, the state's total net load[1] profile was forecast to be defined largely by residential building loads and potentially electric vehicle charging with peak loads occurring in morning and evening hours [Wei et al., 2013b].

This “duck” curve has already been exemplified with net load data collected in 2014 by the California Independent System Operator (CAISO) [Alston et al., 2017]. With increased photovoltaic (PV) and wind energy, California must address significant challenges with system wide resource adequacy, power quality and grid reliability created by variable, non-controllable sources of generation. Conventional power plants were historically adjusted to meet instantaneous or variable demand. With the addition of renewables, CAISO must now maintain reliability by matching the demand for electricity with supply using a variety of measures that adjust electricity production to meet changes in electricity demand on a second-by-second basis [CAISO, 2016]. In a demand response (DR) study conducted for the California Public Utilities Commission (CPUC), four service categories (shape, shift, shed, and shimmy) were evaluated to assess the potential of DR in 2020 and 2025 to support reliable grid operations over different requisite time scales [Alstone et al. 2017]. Load shape, shed, and shift strategies address the need to achieve a more balanced load shape across the day with slow ramped transitions to turn on or shut off generation resources to meet demand. Load shed (dual use term) and shimmy strategies address the need to more quickly respond to system wide shortfalls and rapid changes in demand as an ancillary service.

The DR study quantified the amount of controllable DR that could be expected to be available in 2020 and 2025 across a range of competitive levelized costs for supplying the DR resource, where costs were defined by equivalent procurement costs for an alternative resource that could meet the same needs as DR [Alstone et al. 2017] or incentives linking DR with a value stream for the service. In the simulations, the residential building sector was incented to control loads using time-of-use and critical peak pricing rate structures, whereas the commercial building sector was incented using a time-of-use rate structure. A portfolio of controllable end use technologies were selected based on levelized cost for the DR resource, whether the service could be aggregated to produce reliable DR resource, speed of response (seconds, minutes), level of disruption to operations or occupants, and ability of the dispatchable technologies to provide real time, runtime information and metered data in order to participate in supply side markets. Cost competitive DR load reductions per DR service category were given for the modeled technology measures; e.g., commercial lighting was projected to provide 156 MW-yr of shed DR and 216-303 MW-yr of shimmy DR whereas commercial variable frequency drives were projected to provide 59 MW-yr of shed DR, 3643-3749 MWh-yr of shift DR and 3-9 MW-yr of shimmy DR. The DR study acknowledged that the technology options that were modeled were not comprehensive, that the DR study overall was the first of its kind and could not capture all potential energy scenarios, and that the results were indicative of DR potential.

[1] “Net load” is defined as the sum of demand for electricity and supply provided by renewable generation.

In terms of policy, the CPUC bifurcated the DR program portfolio into 1) "load-modifying" DR resources that shape or reduce the net load curve through price response or behavioral campaigns with advance notice of months to days, and 2) "supply DR" sources that are controlled or dispatched within the CAISO markets [Alstone et al. 2017, CPUC Decision D.14-03-026]. In 2015, the CPUC defined the pathways for valuation of supply and load-modifying DR, where the latter could only provide capacity value through CEC load forecasts for resource (generation) adequacy planning (CPUC Decision 15-11-042). Valuation, however, is further complicated by the interactive effects of energy efficiency and demand response. Energy efficiency investments in controllable technologies could provide both load-modifying DR and the ability to participate in supply DR. The DR study indicated that development of appropriate valuation of such technologies would require careful alignment between CPUC policy and market transformation programs.

Given this context, there is some uncertainty as to whether the dynamic facades industry should develop products that are responsive to California's net load profile, whether such capabilities will be incentivized by utility and non-utility actors (e.g., aggregators, advocacy groups), and whether such products can deliver significant benefits above and beyond that of state-of-the-art controls. Dynamic facades however have the ability to lower heating loads in the morning and evening through solar admission, lower cooling and lighting loads in response to time-of-use rates, and support shifting of loads in combination with precooling strategies by minimizing solar gains during peak periods. When used in combination with advanced heating, ventilation, and air-conditioning (HVAC) and lighting systems, dynamic facades have the potential to deliver very low energy use and demand in perimeter zones, serving as the first line of defense between the highly variable outdoor environment and the indoors. While some measures can result in degradation in delivered service and amenity in buildings, dynamic facades have the potential to enhance the quality of the indoor environment through provision of daylighting and views, improve comfort, potentially increase health and productivity of occupants, while contributing as a net energy producer to the utility grid. With advances in material science and controls R&D likely to significantly reduce the cost of dynamic facades, the sum of the benefits including increased demand flexibility could tip the balance to more widespread market adoption.

This study explores the technical potential of dynamic facades to increase commercial building energy efficiency and provide load shed, shape and shift DR capabilities in support of California's 2050 GHG reduction goals. The objectives of the study are to 1) better understand DR response capabilities of dynamic façades, and 2) enable a more informed dialog to occur between utility actors and the dynamic facades industry in defining the role of this technology within the energy efficiency and demand response context of California. A variable-transmission, three-zone electrochromic window, dimmable lighting, and an HVAC system's thermostat are controlled using model predictive controls (MPC) to minimize energy cost based on time-of-use rates and subject to comfort constraints. A south-facing perimeter zone in a prototypical large office building is modeled using a workflow involving Radiance [Radiance, 2018] and Modelica-based [Modelica, 2018] simulation tools. HVAC and lighting energy demand are evaluated for two climate zones in California. We then discuss the technical potential of MPC to achieve load-modifying DR response and associated cost savings compared to state-of-the-art controls.

2. Background

There have been numerous studies conducted to evaluate the technical potential of HVAC and lighting control strategies to shed and shift loads but very few involving dynamic facades and no known studies that disaggregate savings from combined measures. One extensive simulation study [Gyalistras and Gwerder, 2010] found that integrated control of multiple building systems using optimal predictive control had a 16-41% annual energy savings potential for commercial buildings in Switzerland over the same systems controlled using best available rule-based controls. Savings were due mainly to control of the exterior window blinds, free cooling, and energy recovery. Predictive control of the loads from dynamic facades (i.e., admission or rejection of solar gains) enabled efficient pre-heating or cooling of thermal mass, avoided frequent switching between heating and cooling, and kept room temperatures within the designated comfort range. During the winter, use of heating was avoided in morning hours

by opening the blinds to make better use of incident radiation for pre-heating the room, or alternatively, cooling energy use was reduced by opening the blinds at night to pre-cool the room radiatively prior to solar and internal gains expected for the next day. On summer days, solar gains were reduced to a limit so as not to adversely affect lighting energy use savings from daylight. Use of predictive controls enabled complete avoidance of mechanical cooling whereas rule-based controls resulted in the typical Gaussian load shape profile proportional to outdoor solar radiation levels on sunny summer days. Predictive control of transmitted solar radiation also enabled the mean radiant temperature of the room to remain within comfortable levels in support of the pre-cooling strategy. In all scenarios investigated, the study assumed use of automated blinds so isolating savings due to the blinds was not possible.

Quantifying technical potential from systems integration is challenging, particularly when involving model predictive controls (MPC). With MPC, a model of system operation, along with forecasts of disturbances, is used to predict future performance and optimize setpoint schedules and/or control inputs over a specified time horizon. The solution of the first control step is implemented and the optimization is solved again with updated information (system state and disturbance forecasts) for the next control step. When the controls involve multiple systems, the optimization problem can become complex with prediction horizons of 24 h or more. In prior research, [Coffey 2012] used model predictive controls to determine how to control the dynamic facade and radiant slab heating and cooling system to minimize cooling and lighting energy use over a prediction horizon of 24 h and within zone temperature constraints (20-24°C). The study used reduced-order models for the control optimization, where the models for daylight level, solar gains to the slab and zone air, and thermal aspects of the model were calibrated using an error minimization process to match an EnergyPlus model of the American Society of Heating, Refrigerating and Air-Conditioning Engineers (ASHRAE) 90.1-2010 compliant large office reference building. The optimization was solved with genetic algorithms using GenOpt [GenOpt 2018] then the reduced order models were used to determine final perimeter zone energy use (EnergyPlus could not be used due to inherent limitations of the tool). With MPC control of an exterior or interior venetian blind and thermostat, annual energy use due to HVAC and lighting was reduced by 3-7% for south and west facing perimeter zones in Sacramento, Chicago, and New York compared to the same blind held at a static slat angle (emulating a manually-operated blind).

Interest in MPC has increased given both the desire for more energy-efficient, integrated systems and increased computational power of embedded controllers. Although used extensively in the chemical process, aerospace and transportation industries, MPC is still in the relatively early stages of development in the buildings industry. Experimental studies have been limited to no more than a few dozen proof of concept tests, often in unoccupied test rooms or with HVAC equipment in occupied buildings over a short term period (3 hours to up to 90 days) [Sturzenegger et al., 2016]. Conclusions from these studies indicated that the costs for model development and engineering were too high to justify use of MPC, but that these costs could be reduced significantly if progress was made to develop an MPC software framework and supporting modeling tools.

These development costs are being addressed explicitly by related research. The Lawrence Berkeley National Laboratory (LBNL) has been working to develop such an open source framework based on Modelica modeling and optimization in JModelica.org [Åkesson et al. 2009] that enables real time testing of MPC for buildings, either in real-time connected to a building or, for development and performance testing, in simulation with an emulated building model controlled by the MPC controller, called MPCPy [Blum and Wetter, 2017]. A key focus of this development is to allow the use of reduced order models and simplified HVAC models, with a supporting library of MPC models being developed in collaboration with the International Building Performance Simulation Association (IBPSA) Project 1 [IBPSA 2018]. The objective of this framework and library is to make it easy for non-experts to quickly build a model for MPC that is then adapted during operation based on measured data, thereby significantly reducing setup time and required expertise. Real-time use of this framework for field testing in full-scale testbeds and monitored building demonstrations is now underway within LBNL. The U.S. Department of Energy's (DOE) Building Technologies Office (BTO) has also been supporting tools that would enable energy analysis of MPC-

based technologies through the transformation of its building energy simulation tools [SOEP, 2018]. DOE also recently started supporting development of test emulators and procedures for advanced control sequences including MPC in collaboration with IBPSA Project 1 [Blum et al. 2019].

This study is an extension of prior breadboard prototyping and field testing research and development activities. Under synergistic DOE and California Energy Commission (CEC) supported research, LBNL developed and tested autonomous[2] MPC controls for dynamic facades, then field tested the controls in the LBNL full-scale, outdoor, Advanced Windows Testbed to validate the underlying models, observe operations, and improve performance [Gehbauer et al., 2017; Coffey et al., 2012]. The present solution (described in Section 3.1) involves MPC algorithms that can be configured (and reconfigured at any time over the life of the installation) with a few inputs using a web-based interface then executed on low-cost distributed embedded controllers (e.g., Raspberry Pi). A non-linear optimization solver is used to determine the tint states of a three-zone electrochromic window (i.e., window subdivided into three equal height horizontal bands that are controlled independently) at a 5-min time step over a 24-h prediction horizon using real-time sensor, weather forecast, and utility price data. The 5-min control time step was chosen based on typical dynamics of the sky, impacting the visual comfort of the occupant, i.e., the rate of change in glare and tolerability of intermittent discomfort. The 24-h prediction horizon was chosen based on a daily cycle of operation, where a continuous actuation of the thermal mass of the building was implemented, i.e., the initial state of charge of the thermal mass should be close to the final state of charge. The control objective is to minimize time-of-use energy and demand cost (due to HVAC and lighting loads) within visual and thermal comfort constraints, with added penalties for outcomes that diminish daylight quality and view. The solution relies on open source tools (Modelica, JModelica.org, Radiance) and the MPCPy open source framework.

3. Method

Simulations were conducted to evaluate the performance of an MPC controller relative to conventional manually-operated shades and heuristic, rule-based control of a dynamic facade. The following sections describe the MPC controller (Section 3.1) and "emulator" (Section 3.2) used to simulate the energy and non-energy performance of the state-of-the-art and MPC controllers. Details of the modeled south-facing perimeter zone in a prototypical large commercial office building are given in Section 3.3.

3.1. Controller

This section outlines the latest advancements of the Dynamic Facade Control (DFC) agent, as part of the previously introduced agent-based control architecture for dynamic facades that was demonstrated to be feasible for real-time control in a full-scale outdoor testbed [Gehbauer et. al., 2017]. The DFC agent includes the MPC controller and supporting control modules that enables the advanced control of dynamic facades, such as electrochromic windows, within an optimization framework. Challenges for developing the agent were a) integration of the complex fenestration models required for accurate daylighting, solar heat gain, and glare calculations, and b) development of the overall control architecture needed to seamlessly integrate the MPC controller into existing or new buildings. Both of these challenges were addressed in the 2017 study. The resultant DFC agent allows the addition of user constraints such as desired glare level, time-varying work plane illuminance setpoints, occupancy schedule, temperature setpoints for heating and cooling, and previously set maximum demands for time-of-use (TOU) optimization. It accepts external data (sensors, weather forecasts), performs the optimization, then determines the control state of the devices for actuation. The DFC agent was integrated with an "emulator" i.e., gold standard, validated building energy simulation engine (Section 3.2), where inputs and communication were modeled as in a real-world deployment enabling Controller-in-the-Loop (CIL) testing. The following subsections describe the

[2] "Autonomous" = Facade controlled for HVAC and lighting energy cost minimization but without explicit real time data exchange for control.

implementation of the DFC agent, integration of the Radiance tool in the MPC controller within the DFC agent, and the optimization workflow used to determine the optimal state and setpoints for final actuation.

In this study, the control objective of the DFC agent was to minimize total energy cost based on California time-of-use energy and demand rate schedules for large commercial buildings.

3.1.1. Implementation approach

The Dynamic Facade Control Agent is written in Python and implemented as a set of utility functions, wrapped in a class. This top-level class *mpc_controller* includes the instantiation of sub-modules necessary for control, including Radiance, JModelica.org, and PyFMI [PyFMI, 2018]. While PyFMI is a Python package for the interaction of models conforming to the Functional Mockup Interface (FMI) open standard [FMI, 2018], JModelica.org is a tool for the compilation, simulation, and optimization of Modelica models with a Python API, and Radiance is a stand-alone tool for daylight analysis which is wrapped with a number of Python utility functions. After instantiation, the class is queried using a syntax similar to the FMI standard. An external trigger class handles the real-time control of the agent to ensure timely control steps, which are set to 5-min intervals. On a trigger event the *do_step* function is called to query the control, and compute the control for the next time step by taking a 24-h prediction horizon into account. In the simplest case *do_step* only requires the current trigger as datetime format. However, depending on the configuration, further inputs such as previously set demand charges or building occupancy may be provided. Figure 1 shows the process flow of the triggered controller.

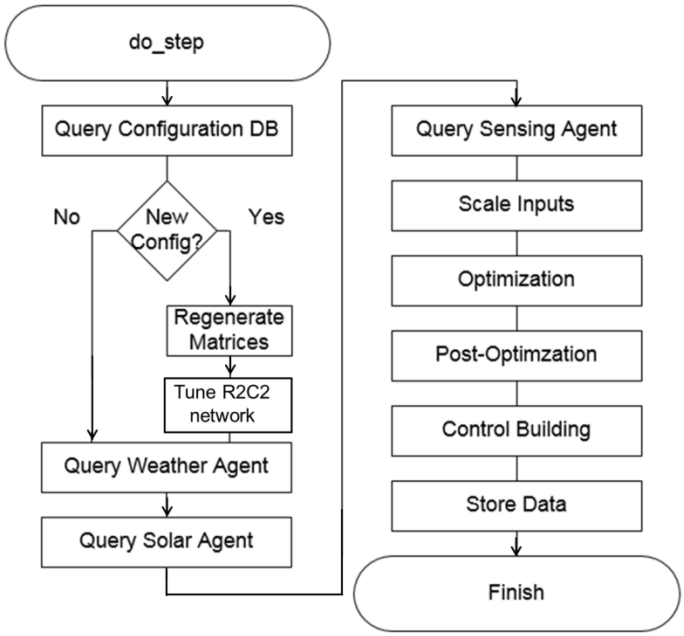

Figure 1. Process flow of Dynamic Facade Control Agent.

Steps for the process flow are as follows:

1. The control step starts with a query of the zonal database to get the room configuration; e.g., dimensions, occupant view direction, site location, etc. If a change in any of these inputs is detected then the matrices and configuration files for Radiance are recomputed.

2. The Weather Forecast agent is queried to get the latest 24 h weather forecast of global horizontal, diffuse horizontal, and direct normal irradiation. The hourly forecast is then interpolated to match the current timestep of triggering, and used as input for Radiance to compute parameters related to the fenestration system. These forecasts include work plane horizontal illuminance (WPI), solar heat gain (SHG), and vertical illuminance (Ev) for each window zone and for each timestep of the forecast. The vertical illuminance quantity is used to calculate the simplified daylight glare probability index (DGPs, [Wienold, 2009]) at the occupant's viewpoint.
3. If real-time data from a solar sensor is available, then the Real-time Solar agent is queried to get the latest measurements. These measurements are used to produce more accurate predictions, but only for the current timestep, and then passed to a function which scales the whole 24 h forecast, increasing the accuracy of the weather forecast.
4. The last input queried, if it exists, is the Sensing agent which can provide additional updated state measurements such as room air temperature, occupancy, or HVAC status through the building management system (BMS).
5. Construction details of the modeled zone are assumed to be unknown, so if the timestep is at the beginning of the hour, then automated model tuning is conducted to estimate RC parameters for the room load calculation (see Section 3.1.2.3.6). Additional options allow inputs to be scaled or otherwise modified by a machine learning (ML) model, such as Random Forest, or Artificial Neural Networks, which enable self-commissioning, self-calibration, and self-adaptation. However, these options were disabled for this simulation study.
6. The next two steps of optimization and post-optimization are the computation of the control signal and are further described in the sections below.
7. The control states or setpoints from the optimization are communicated with actuators of the dynamic facade and building by the Control agent.
8. As a final step, all input and output information are stored in a Python-based database to record historic trends for debugging and to support ML models.

3.1.2. Optimal control

The concept of the introduced control uses an MPC approach where a model represents the physics of the system and an optimizer explores global optima of control inputs. These models for optimization are complicated to develop and involve several decisions with regard to complexity, linearity, continuity, and accuracy. This is where the developed tool chain engages to significantly simplify this process.

3.1.2.1. MPC tool chain

MPCPy is part of a tool chain to abstract these modeling details by providing a simpler user interface in Python to automatically generate optimization problems from Modelica models, as shown in Figure 2.

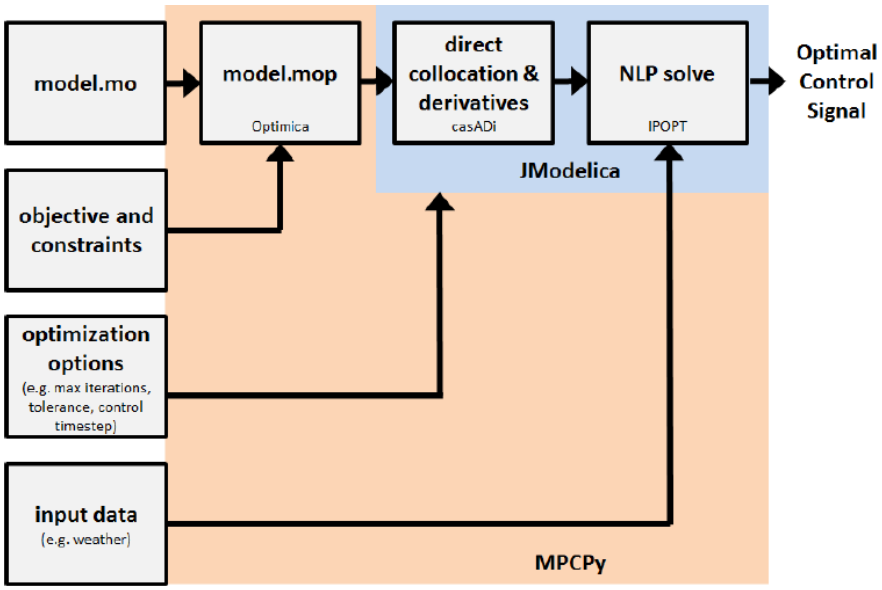

Figure 2. Model Predictive Control tool chain to optimize a Modelica model.

The modeling starts with the commissioning or implementation of a model which represent the physics of the building. This could be a single window, a thermal zone, or a building with multiple zones. It is generated using Modelica and stored in the *.mo* file format. MPCPy facilitates the linkage between the Modelica model and JModelica.org by adding additional equations which represent the objective function (e.g., energy minimization or energy cost minimization) and constraints (e.g., temperature bounds for thermal comfort or limiting equipment capacities). By doing so, it converts the Modelica *.mo* file into an Optimica *.mop* file. In the next step, it passes the Optimica file to JModelica.org where casADi [Andersson et. al., 2012] is used for the automated differentiation of equations and transfer to a non-linear optimization problem with direct collocation. Finally, the problem is handed to the non-linear problem (NLP) solver IPOPT (Interior Point Optimizer) where it is used with the MA27 linear solver [HSL 2019]. IPOPT [Wachter and Biegler 2006] is the default solver out of a few supported solvers in JModelica.org and is designed to find local solutions for constrained NLP [IPOPT, 2018]. However, when provided with a convex problem then IPOPT should find the global solution. Due to the nature of most NLP solvers, IPOPT requires all variables to be continuously differentiable for the first and second derivatives. This means that no discrete states, such as on/off binary variables or integer variables, are allowed. This potentially reduces the application of NLP solvers for HVAC control systems, where discrete control states are often used in logical IF conditions. However, to an extent, models can be reformulated to approximate the real system behavior.

3.1.2.2. Method

Controls based on MPC are typically used as slow-acting supervisory controllers, as they exploit the information from many sources to make global strategic decisions. Such supervisory knowledge is especially useful when optimizing for time-of-use rate structures, where a single 15-min peak defines the cost of demand charges for the entire month. Other MPC applications are those that have large time constants; e.g., a radiant slab, the chemical process industry, or applications where control has a high impact on the objective; e.g., shifting peaks from high price periods where mass must be charged in advance [De Coninck and Helsen, 2016] or start up of power plants [Sällberg et. al., 2012]. However, real-time, near-instantaneous control is typically conducted by a separate controller with different objectives. The approach in this project is to use MPC control as the real-time controller by implementing a fast-acting optimization, ultimately resulting in more optimal operation. The challenge with this approach is the convergence time of the optimization, which increases exponentially with the number of timesteps

and complexity of the problem. In a first implementation the convergence time was greater than the desired timestep for control. In order to avoid long, intensive optimizations, a multi-stage MPC framework was developed where the workload was separated into a supervisory *major* optimization and a *minor* optimization, enabling real-time control (i.e., timesteps faster than 1 min).

The *major* optimization, with a 24 h horizon and hourly time step, is computed first and the optimal result for the next hour is used as a target for the *minor* optimization, with a 1 h horizon and 5 min time step. The result from the *minor* optimization is implemented as real-time control; i.e., major and minor optimizations are performed each 1 min in order to respond quickly to glare but address energy cost minimization over the 24 h horizon. This method can be described as a "zoom" function, where supervisory setpoints are passed to lower level optimizations with the same objectives, enabling smaller time steps to be implemented in the building in real-time. While this process requires two separate optimizations, the problems are much smaller, i.e., 24 and 12 timesteps respectively, in comparison to a single 24 h optimization with 5 min timesteps, totaling 288 timesteps. An example of the typical number of iterations and convergence times for a single day of field operation is shown in Figure 3.

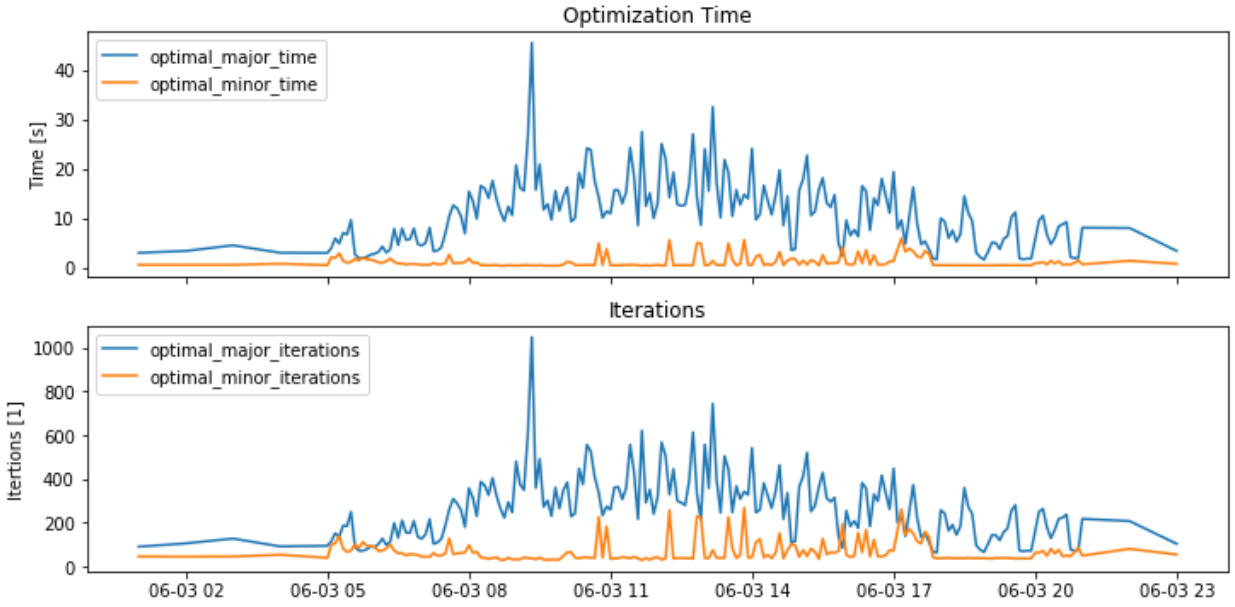

Figure 3. Typical convergence time and number of iterations before achieving convergence for the minor and major optimizations on a single day (June 3).

It can be seen that the number of iterations and corresponding convergence time required increases for the *major* and *minor* optimization between nighttime, when conditions are relatively stable, and daytime: i.e., from 3 to 20 s and 0.5 to 2 s, or 90 to 400 iterations and 50 to 100 iterations, respectively.

3.1.2.3. Implementation

The optimization uses the same base Modelica model and control architecture previously described in [Gehbauer et. al., 2017], but with some modifications to the penalty functions. Figure 4 shows the updated model used in this study.

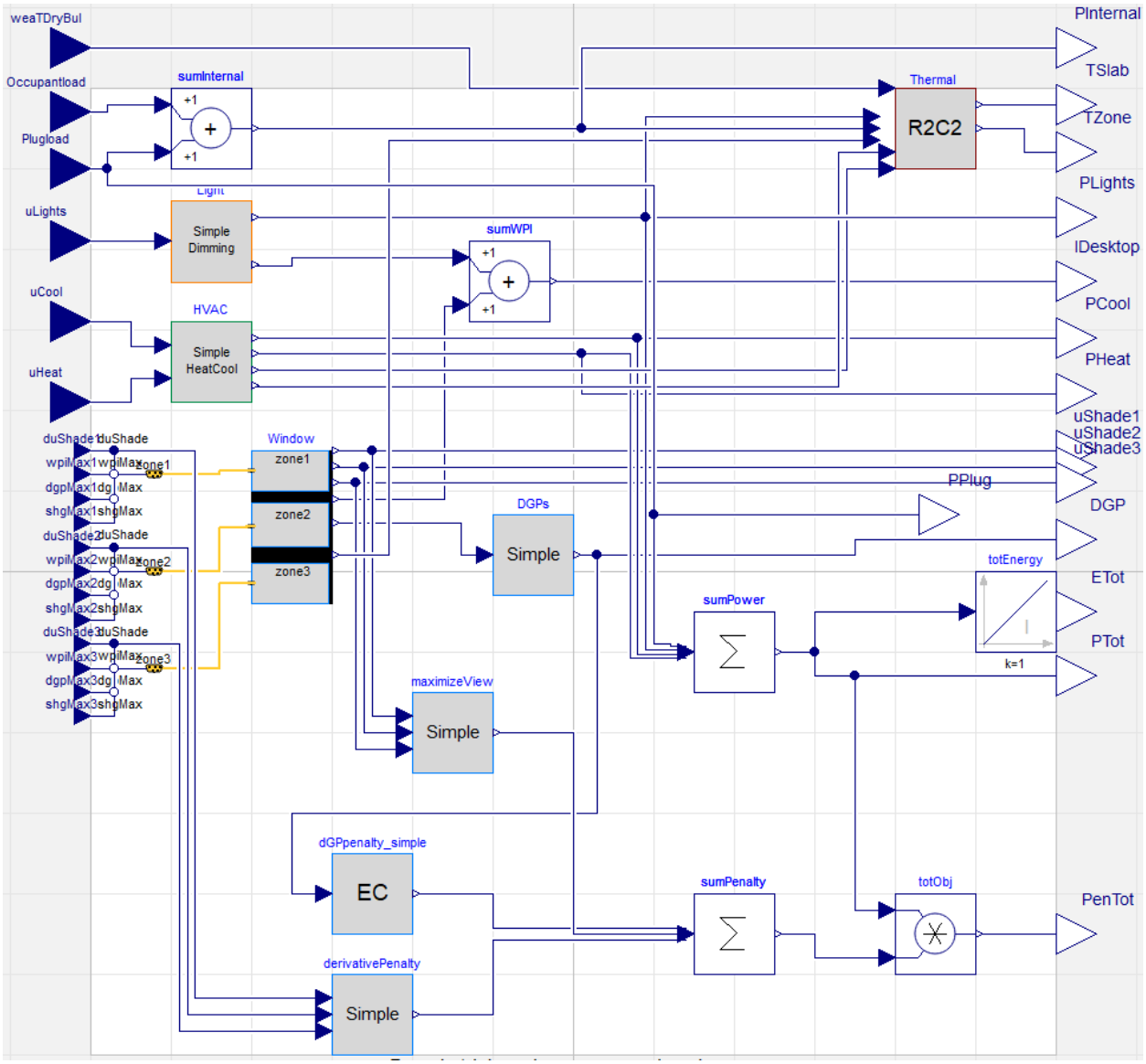

Figure 4. Updated Modelica model used for Model Predictive Control.

The room model consists of a number of sub-models, 17 time-varying inputs, and 12 outputs, as described in [Gehbauer et. al., 2017]. The inputs are:

- Outdoor dry bulb temperature, in degrees Kelvin
- Plug loads and internal gains (including people), in Watts
- Lighting control signal, as a continuous signal from 0 to 1
- Cooling control signal, as a continuous signal from 0 to 1
- Heating control signal, as a continuous signal from 0 to 1
- Clear window state inputs of the dynamic facade for WPI, SHG, and DGPs for each window zone, as determined by the Radiance three-phase method
- Derivative of window control signals, which are optimization variables

Additions to the base model are a) the combination of the maximize daylight and view penalty, b) a re-definition of the DGPs penalty function, c) a derivative penalty, and d) the separation of electric power and penalty outputs. An addition to the converted Optimica model is the integration of a time-of-use cost module. These additions are described as follows.

3.1.2.3.1. Maximize view penalty

The function to penalize tinted states to allow for a better daylighting and view was revised to a single equation for all windows:

$$Pen_{View} = n_v * \sum_{z=1}^{3} Tint_{Clear} - Tint(z) \quad (1)$$

where n_v is the gain of the function, z is the window zone index, $Tint(z)$ is the tint level (real number between 1 and 4), and $Tint_{Clear}$ is the maximal tint state (i.e., 4). This formulation simplifies the problem while providing the same capability to tune the level of disruptive tinting.

3.1.2.3.2. DGPs penalty

The DGP penalty was revised due to long iterations, frequent infeasibilities and general complexity of the resulting problem. It was revised from a 22nd order exponent to a 10th order exponent by:

$$Pen_{DGP} = n_g * (DGPs - offset)^{exponent} \quad (2)$$

where n_g is the gain of the function, *DGPs* is the currently experienced glare level, *offset* is an offset to shift the penalty from regions with unacceptable glare, and *exponent* is the exponent of the penalty, describing the steepness of the gradient, with a typical value of 10. This modification significantly reduced the iteration time and increased the ability to find solutions. One explanation is the NLP optimization performed by JModelica.org was having difficulties handling steep gradients in non-convex problems that lead to local solutions.

3.1.2.3.3. Derivative penalty

The derivative penalty was introduced to dampen the operation of tinting to avoid disrupting the occupant. It required changing the shading input from a control signal (e.g., 1-4) to derivative signals with a starting point (e.g., 4), and then temporal derivatives, denoted as $d(Tint(z))/dt$, to operate the dynamic facade. The resulting formulation of the penalty function is:

$$Pen_{Der} = n_d * \sum_{z=1}^{3} \left(\frac{dTint(z)}{dt}\right)^2 \quad (3)$$

where n_d is the gain of the function, and the squared term is the derivative of the window zone throughout the optimization horizon.

3.1.2.3.4. Separation of outputs

In an initial implementation, the output was a single objective function variable, which lumped the electric power consumption and penalty function together into a single value. This was problematic because TOU rates are very sensitive to peaks, potentially distorting the impact of the penalty functions. It was therefore necessary to separate the outputs into electric power consumption and penalty values to allow accurate assignment of TOU rates only to the electric power consumption.

3.1.2.3.5. Time-of-use cost model

Most commercial tariffs in California consist of two elements: the cost for energy in \$/kWh and the cost for peak demand in \$/kW. MPCPy was extended to add the cost of demand for a user-specified number of periods, which is typically three periods in summer and two periods in winter. The general form of the monthly utility bill calculation is described by Equation 4 in discrete time, with B in units of dollars (\$):

$$B = \sum_{t=0}^{m}\left(\pi_{e,t} P_t \Delta t\right) + \sum_{\tau=1}^{q}\left[\pi_{d,\tau} \max(\bar{P}_\tau)\right] \quad (4)$$

Here, the first term represents the energy cost over the month from time, t, from 0 to m. In the first term, $\pi_{e,t}$ is the cost of energy at time t, P_t is the power consumption supplied to lighting, cooling, heating, and plug loads at time t, and Δt is the time discretization interval, assuming that P_t is constant over each interval. The second term of the cost represents the sum of demand costs over a number of periods, τ, from 1 to q, where each period is defined by certain hours within the days of the month. The demand cost in each period is equal to the price of demand of the period, $\pi_{d,\tau}$, times the maximum of the power consumption during the specific times of the period, which is a vector $\bar{P}_\tau$. While this is the calculation of the utility bill over the month, it is impractical to optimize an entire month of performance at each control step. Therefore, the Equation 5 is transformed into the control optimization Problem Y to be solved at each control step:

$$\min_{P,z} J = \sum_{t=t_o}^{t_f}\left(\pi_{e,t} P_t \Delta t\right) + \sum_{\tau=1}^{q}\left(\pi_{d,\tau} p_\tau\right) \quad (5)$$

$$s.t.$$

$$P_t \leq p_\tau + \hat{p}_{t,\tau} \text{ where } \begin{cases} \hat{p}_{t,\tau} = p_{est,\tau}\,, \forall t \in \tau, \forall \tau \\ \hat{p}_{t,\tau} = M\,, \forall t \notin \tau, \forall \tau \end{cases} \text{ and } M \gg 1$$

$$p_\tau \geq 0, \forall \tau$$

Problem Y states that we seek to minimize J by controlling P and p. Here, the first term of the objective is similar to that of Equation 4 and represents the energy cost for the specified time horizon t_0 to t_f. In the second term of the objective, we have performed a change of variable from Equation 4, where we replace the max function for each period with the variable p_τ and add a constraint that P_t (excusing the added variable for now) must be less than p_τ for each t in the period τ, resolving that $p_\tau$represents the max of P_t during each period. A second constraint requires that $p_\tau$be non-negative.

We face two additional issues to resolve using this formulation. The first is that specifying a dynamic control problem in Modelica and Optimica, prior to time discretization, P_t is actually a continuous function of time $P(t)$, and so we need to enforce the constraint with p_τ only for times during the period, and otherwise hold no constraint on $P(t)$. For this, we add $\hat{p}_{t,\tau}$, which is defined as a constant for times during the period and a very large number, M, otherwise, thereby only enforcing the constraint at times during the period.

The second issue is the fact that for a given month, the demand costs are to achieve a specified ratio to the energy cost. However, during a single time horizon of the MPC, say 24 h, the cost of demand will disproportionately outweigh the cost of energy over that time, since it is only one day's worth of energy, rather than a full month's worth. Therefore, we must make the constant $\hat{p}_{t,\tau}$ equal to an estimation of the peak demand during that period for the month, $p_{est,\tau}$, which may either be a peak that has already been achieved during the month, or is predicted to be

achieved during the month in later days. We note that in doing this, p_τ becomes the difference between the peak power during the time horizon and the estimated peak for the month. If $p_{est,\tau}$ is very high, the constraint is always true, and the optimal p_τ will reduce to 0, indicating that no additional cost will be added for demand during the time horizon for that period. This makes sense, since the peak demand for the month for that period may have already been set by $p_{est,\tau}$. If $p_{est,\tau}$is very low, the constraint will be enforced at the optimal, with the optimal p_τ reducing to the difference between the maximum of P_t and $p_{est,\tau}$. This also makes sense, as the impact of demand on the objective function will only be the additional cost of increasing the peak demand for the month by p_τ. That is, only the marginal demand cost for each period during the time horizon is added to the energy cost of the time horizon.

Viewing the energy cost of the time horizon as the marginal energy cost for that time horizon for the month, we notice that the resulting objective of Problem Y is to minimize the marginal cost of energy and demand. The demand charge is applied to the peak 15-min period of the whole month, whereas the optimization horizon is typically less than this (e.g., 24 h in this study). It is therefore advantageous to estimate the monthly peak demand to utilize available capacity for energy shifting, rather than demand reduction, if the peak demand is forecasted to occur sometime after the optimization horizon. In Cutsem et al. 2019, the performance of including forecasted or already occurred peak demand was compared to one that took into account energy prices only (no demand charges), and to a more conventional one that considers the energy prices and demand cost at each optimization horizon. The case study simulated the performance of office buildings (modeled simply) operating under two California tariffs with demand response events induced by critical peak pricing. The study also compared the performance of the incremental formulation with and without estimations of peak demand. The study found that the incremental demand formulation slightly reduced the monthly utility bill for the customer compared to the full demand, but significantly improved the energy-shifting responsiveness of the buildings to peak energy pricing during demand response events. Accurate peak estimation only slightly further reduced the utility bill and improved energy shifting response, particularly in the beginning of the month. However, while the option of incremental demand consideration was built into the controller, this initial study did not forecast monthly peak demand, hence this functionality was not utilized, and the full demand charge was added to the 24 h optimization horizon.

3.1.2.3.6. Parameter estimation for the RC network

The thermal response of the zone is modeled using a second-order resistance-capacitance (RC) greybox model, known as an R2C2 model, and is written graphically in Modelica (Figure 5). This model accounts for thermal mass effects by separately accounting for zone air volume thermal capacity and zone internal mass thermal capacity, which operate on faster and slower dynamic timescales, respectively. This also accounts for the fact that the HVAC system has no direct activation of internal mass in an air-based system, requiring all charging and discharging to come as a result of temperature differences between the air and the mass. Note that the HVAC heating and cooling powers are assumed to be 100% convective gains, while the internal heat gains are split between radiant and convective powers in accordance with a set of parameters k_n. These parameters are either statically (at initialization) or dynamically (periodically at runtime) estimated using data from the building. Each input to the R2C2 model is assigned to a first-order calibration function, which can compensate for model errors from previous steps (i.e., Radiance for WPI and SHG, equipment load, and occupancy forecast).

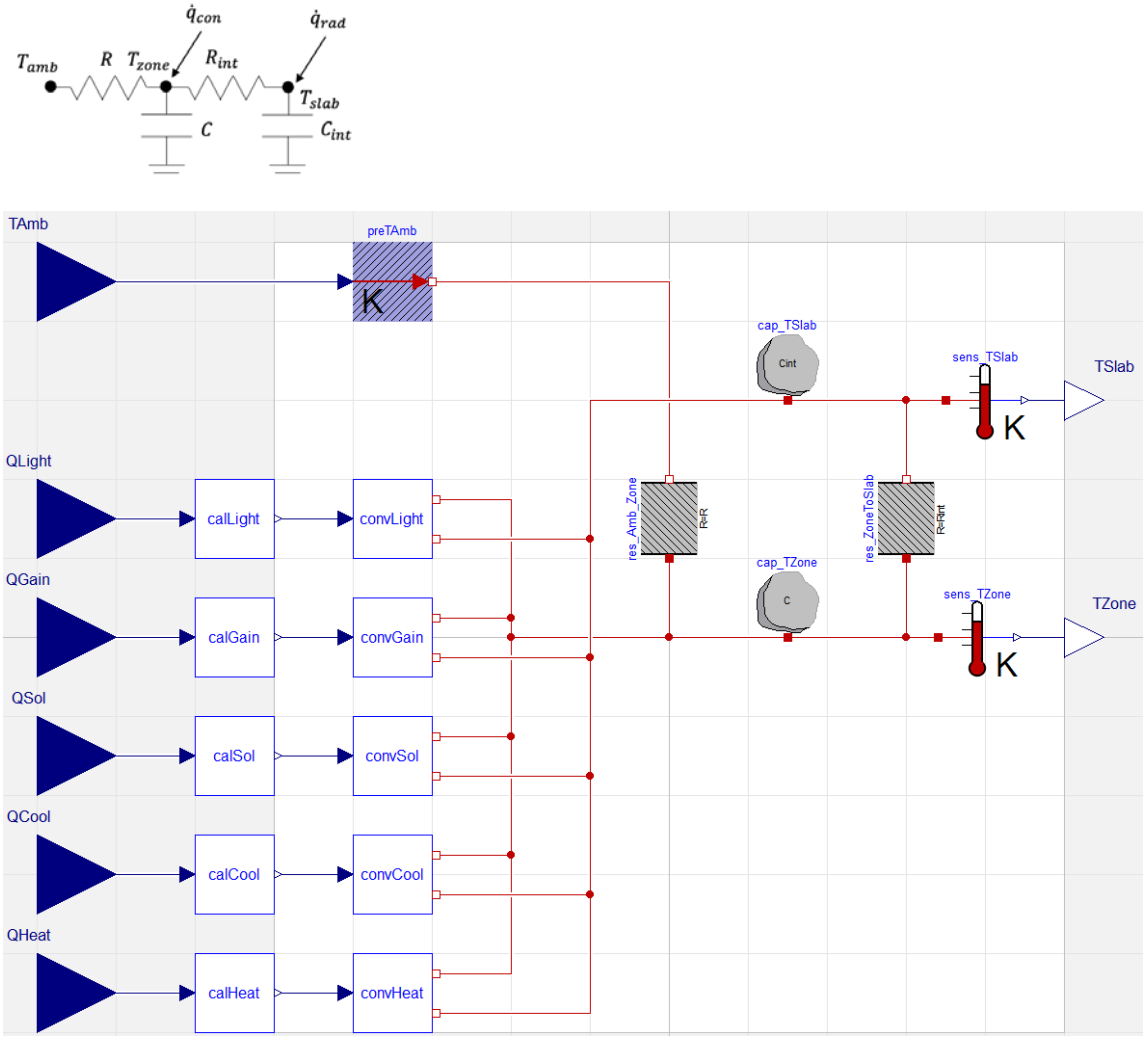

Figure 5. R2C2 schematic diagram (above) and R2C2 model implemented in Modelica (below).

The model parameters were tuned at the beginning of each hour using an optimization-based parameter estimation technique to minimize the error between modeled and "measured" historic zone air temperature from the detailed emulator model. In this technique, the optimization problem is formulated so that the objective function is the squared error, the optimization variables are the tunable parameters, which are constant over the time period of the optimization, and the constraints are the model equations and minimum and maximum allowable parameters on the tunable parameters. The method was implemented using the JModelica.org optimization package through the MPCPy framework. The parameters tuned were R (resistance of air to outside), Rint (resistance of air to internal mass), and Cint (internal mass capacitance). Note that the air thermal capacity (C) was calculated according to the density of air, specific heat at constant volume of air, and volume of the zone. The prior 24-h period of 5-min measured data from the emulator, along with weather and internal load inputs, were used for the training period.

3.1.2.4. Optimization module

In the simplest case of operation, the controller only requires the current timestep to perform the optimization, and returns an optimal control signal. If desired and available, additional inputs such as occupancy, internal loads, allowable temperature band, or previously set maximum demands, can be dynamically added to increase the model accuracy. The optimization workflow is as follows:

1) The first step is to compute the input tables for JModelica.org which are non-alterable inputs such as weather forecast, Radiance computed window contributions to SHG, WPI, and DGPs, internal loads, and occupancy. Note that the latter two are only added if data are provided by the user.
2) Another table includes the constraints for the optimization, such as minimum and maximum acceptable temperatures, WPI minimum setpoint, maximum DGPs level, and control band definitions for lighting, heating, cooling, and windows. Note that in order to avoid infeasible starting points (e.g., if the initial temperature is already out of the temperature comfort range), the constraints for the first timestep were bound to a deadband around the initial state.
3) If TOU rates are used, then a third table with the applicable rates and the maximum demand charges (determined by prior operations) is provided.
4) Finally, a table with an initial guess of control signals must be provided, i.e., window tint states, and heating, cooling, and lighting control signal. While for other optimization solvers this initial guess is crucial, IPOPT is very robust against initialization as long as the problem has a convex formulation. A test showed that the number of iterations could be reduced by half when providing a near optimal initial guess: by computing the Modelica optimization model as a simulation model. In this study, an external Proportional Integral (PI) controller was connected to control heating and cooling inputs to keep the temperature within the allowed temperature range. While the time savings for the convergence of IPOPT were less than 0.5 s, the computation of the simulation model took several seconds. The current framework was therefore initialized with a static initial guess of zero (or darkest tint state), avoiding the computation time of simulation models.

Once all tables are passed to MPCPy, the *major* optimization is initiated. MPCPy handles all communication with JModelica.org, such as reading and writing of files, and returning the optimal solution. The Dynamic Facade Control agent checks the result for infeasibilities, and if an optimal solution is found, reads back the desired control state of dynamic facade and room temperature for the next hour. These values are then plugged into the constraints table for the *minor* optimization. The *minor* optimization is conducted in the same fashion as the *major* one, then optimal results for the next 5 min are returned to the agent.

3.1.2.5. Post-optimization module

As described earlier in this report, the NLP formulation does not allow discrete variables. The output from the optimization is a continuous value (real number between 1-4; e.g., electrochromic tint state of 3.7), not an integer (discrete state). For some electrochromics (or other types of dynamic facades), the windows can only be controlled to a small number of discrete tint states. To determine the final discrete control value for the windows, a post-optimization module was developed. Parametric simulations (e.g., for all possible combinations between the three window zones and tint states 3 and 4 for an example result of 3.7) were conducted for the first time step of the optimal result. The discrete tint state (Tint 3 or 4) for actuation was then selected based on a set of heuristic IF conditions (Figure 6).

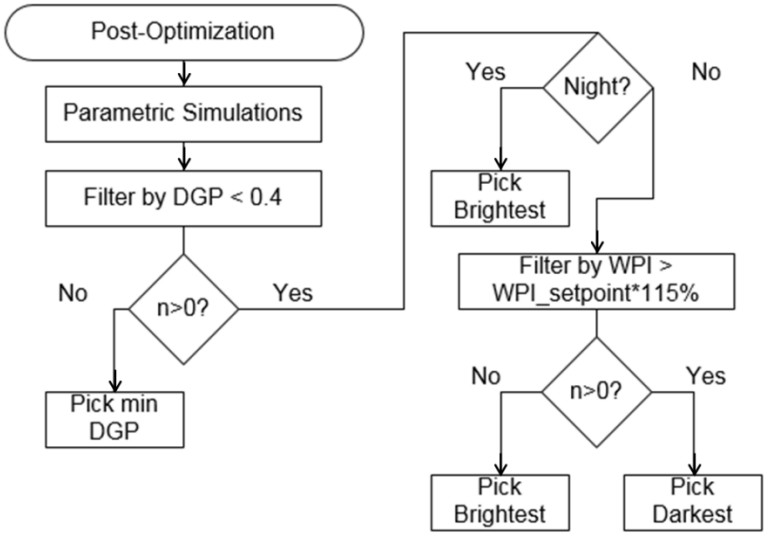

Figure 6. Process flow of post-optimization. The variable "n" refers to the number of remaining control options.

Figure 6 shows the logical decisions made, which can be split into three sections:

1) All cases are filtered for a predicted glare level of below 0.4 (threshold for "disturbing" glare). If none of the cases produce values below the DGPs threshold (i.e., the number of remaining control options *n* is zero), then the case with the lowest glare level is selected.
2) A check is conducted to set the windows to the clear tint state (Tint 4) when the desired WPI setpoint is below 10 lx during the night.
3) The remaining cases are filtered by a predicted WPI level from daylighting that is 15% higher than the setpoint. If such cases exist, then the one with the lowest daylighting level is selected. Otherwise the case with the highest daylighting contribution is selected.

Note that DGPs was computed at a seated eye height of 1.2 m (4 ft) looking normal to the window at a distance of 1 m (3 ft) from the window. WPI was computed across a regular grid at 25 locations in the space, averaged, and used to compute lighting energy use and daylight quality (item 3 in the list above).

3.2. Building emulator

An emulator was developed to simulate and evaluate the performance of rule-based and MPC control of dynamic facade and HVAC systems for a single zone in a building (lighting was modeled to dim independently in response to available daylight or turn off during periods of vacancy). The emulator consists of three main components: 1) controller, 2) detailed zone facade model, and 3) detailed zone thermal model. The detailed facade and thermal model components represent real building performance using state-of-the-art modeling techniques to simulate solar heat gain, daylighting, and zone heat balance physics. The controller uses environmental conditions and the simulated building state to provide shade position control signals (or in this study, electrochromic tint state) and zone temperature setpoints to the detailed models. The detailed facade model takes the shade position control signals and environmental conditions and calculates the resulting glare, daylight illuminance, and solar heat gain components using Radiance. The detailed thermal model takes the solar heat gain components and daylight inputs from Radiance, zone temperature setpoints, environmental conditions, and internal loads and calculates the new perimeter zone/ room thermal state. The thermal model is from the Modelica Buildings Library, which has been validated in separate studies [Wetter et al. 2014, Nouidui et al. 2012a, Nouidui et al. 2012b]. To complete the calculations, the detailed thermal model uses a model developed in Modelica and an MPCPy *systems* object to

export the model as a Functional Mockup Unit (FMU), a model that complies with the FMI standard [FMI, 2018] using JModelica.org, define sources of data for inputs and parameters, and integrate its simulation into the emulator workflow. These components are described in more detail as follows.

3.2.1. Façade model

The detailed facade model uses the Radiance three-phase matrix algebraic method [McNeil and Lee, 2013] to compute the simplified daylight glare probability (DGPs) index, daylight illuminance at the workplane (WPI), and solar heat gain (SHG) contributions from each of controlled zones of the facade system at each time step given inputs from the MPC controller on window or shade position. The three-phase method involves pre-computing view, transmission, and daylight matrices for time-efficient use during run-time. View and daylight matrices are pre-computed for each sensor location and each façade zone (e.g., electrochromic window subdivided into three horizontal control zones). Transmission matrices are pre-computed using the LBNL WINDOW software [WINDOW, 2018].

At each time step, a facade control signal (tint state) is delivered from the controller. The facade model selects the corresponding transmission matrix to compute workplane illuminance, DGPs, and solar loads for each window zone, which are then summed to values for the entire window.

A grid of virtual sensors is generated on each interior surface (facing normal to the surface) to calculate its incident solar radiation. A view matrix is computed for each surface to each window zone.. The average of the grid sensor values is multiplied by the total area of the corresponding surface to represent total incident solar radiation. To calculate absorbed energy at each glazing or shading layer, incident radiation on each surface of glazing and shading layers of the window is determined using the three-phase method then multiplied by the respective bidirectional absorption coefficient of the surface.

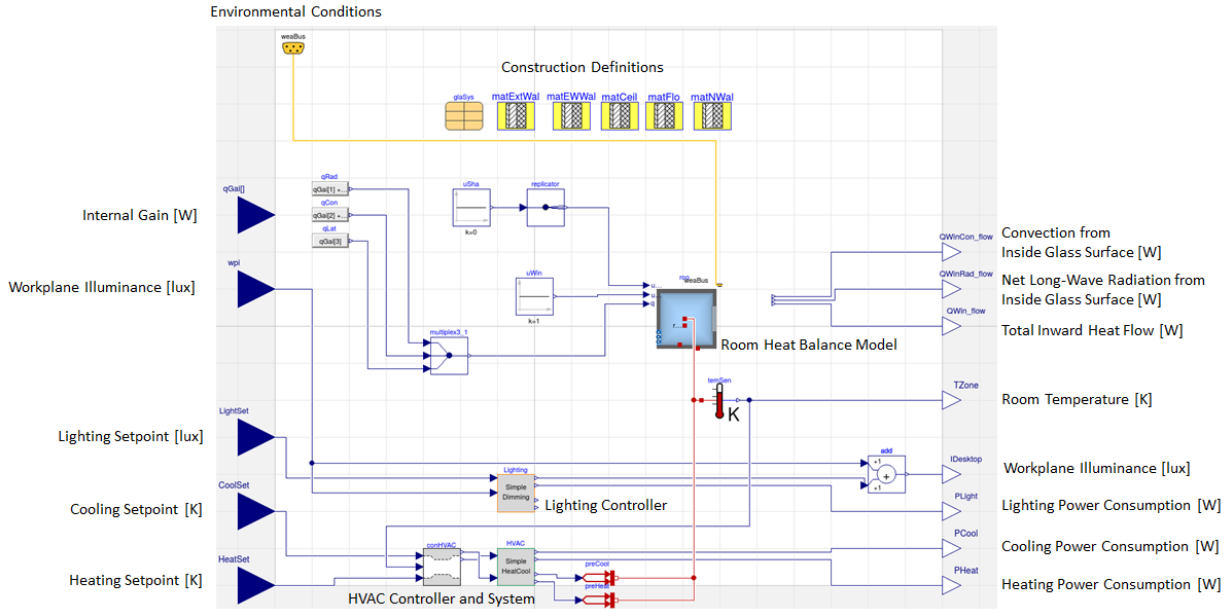

Figure 7. Thermal emulator model in Modelica.

3.2.2. Thermal model

The detailed thermal model, presented in Figure 7, uses components from the Modelica Buildings Library and Modelica Standard Library [Modelica Association, 2013] to perform a room heat balance calculation as well as other supporting functionality. The component models in the Modelica Buildings Library have been individually tested and validated against accepted data and models found in the literature (as cited in Section 3.2). The room heat balance calculation is performed using the *Buildings.ThermalZones.Detailed.MixedAir* component model. It includes building construction properties, orientation, environmental inputs, power for the lighting system, internal heat gains, and heating and cooling supplied by the HVAC system. Supporting functionality of the thermal emulator model includes lighting and HVAC system models and controllers to regulate the room temperature and light level. The lighting system is modeled as dimmable LEDs with linear power consumption. The lighting controller provides the additional light required over daylight illuminance, calculated in Radiance and input to the model, to meet an illuminance setpoint. The HVAC system is modeled as convective heating and cooling, at a fixed coefficient of performance (COP) and efficiency. The HVAC controller utilizes a proportional feedback controller to maintain the room temperature between heating and cooling setpoints. Heating is applied if the temperature is below the heating setpoint, cooling is applied if the temperature is above the cooling setpoints, and the system is idle if the temperature is between these setpoints (deadband).

The window model used within the *Buildings.ThermalZones.Detailed.MixedAir* component, validated by WINDOW 6 and laboratory measurements [Nouidui et. al., 2012] for glazing systems without shades, uses glass properties, solar radiation angle of incidence, and shade position to calculate the transmitted solar radiation through each glass layer, along with the radiation that is reflected by each glass layer and absorbed by each glass layer and the shade. As written in the Buildings Library, for the transmitted solar radiation passing into the room, it is assumed that all of the radiation strikes the floor and is bounced once to all surfaces in the room as a function of their view factors with the floor, including the interior glass layer of the window. The radiation is then absorbed by each surface, including window glass layers, according to the absorptance of the materials and included in the remaining heat balance calculations of the room. A modification was made in this study, however, to use Radiance to compute transmitted solar radiation as described in Section 3.2.1 above for complex shading systems. The modification replaces the variables representing the transmitted solar radiation incident on each surface and absorbed by the glass layers with input variables that are calculated using the three-phase method at each time step.

3.3. Simulation setup

Analysis of MPC performance was conducted on a prototypical south-facing private office using the emulator described above. The prototype was based on the DOE prototype large office building [Deru et al., 2011], updated to comply with the California Title 24 2016 Standard for building energy efficiency [CEC, 2015], and modified to match the zone geometry of the LBNL Advanced Windows Testbed. The large office prototype is a 12-story building with a 73.2 by 48.8 m (240x160 ft) floorplate, where each perimeter and core zone is modeled with adiabatic surfaces. In this study, a single perimeter office zone is modeled as 3 m wide, 4.6 m deep, and 2.7 m high (10x15x9 ft) space with a floor-to-floor height of 3.95 m (13 ft) and 3 m wide by 2.7 m high window (6.78 m^2, 72.9 ft^2 area, window-to-exterior-wall ratio (WWR) of 0.59). The visible surface reflectances of the walls, ceiling, and floor were 50%, 80% and 15%, respectively. The room was unfurnished. The exterior wall assembly had a U-value of 3.9 W/m^2K (0.65 BTU/h-ft^2-°F). The floor construction consisted of a 10 cm (4 in.) thick heavy weight concrete slab with a carpet and pad. Internal loads were due to lighting (installed lighting power density of 8.6 W/m^2 (0.8 W/ft^2)), equipment (10.82 W/m^2, 0.97 W/ft^2), and occupants (0.005 occupants/ft^2). The lighting controls were modeled to respond to occupancy and scheduled events (via the lighting schedule) and dim with an efficiency of 0.24 W/lx to maintain a 350 lx setpoint in combination with daylight at the rear of the perimeter zone. The HVAC system was modeled with a static coefficient of performance (COP) of 4 and heating efficiency of 1. Fan energy was

not implemented. Temperature control was implemented as a PID control loop for heating and cooling with a temperature band from 21.0 to 24.0°C during daytime hours and 15.5 to 26.5°C during night hours from 6 PM to 8 AM local time.

For the automated windows, an electrochromic window was modeled with three, equal height, independently controlled zones. Each electrochromic zone could be switched to a) one of four discrete tint states instantly, or b) as continuously variable between the clear and darkest tinted states. The EC zones were allowed to switch to any state at each time step in this initial study. Center-of-glass window properties for the four discrete states were as follows: visible transmittance (Tvis) range of 0.01, 0.06, 0.18, and 0.60; solar heat gain coefficient (SHGC) range of 0.09, 0.11, 0.15, and 0.41. The U-value of the window was 1.6 W/m^2-K (0.28 BTU/h-ft^2-°F). The base case was defined with low-e, dual-pane windows (Tvis=0.62, SHGC=0.40, U-value=1.6 W/m^2-K) and an indoor fabric roller shade (Helioscreen gray, 3% openness factor, total solar transmittance of 0.044 and front reflectance of 0.27). To emulate a "manually-operated" shade, the shade was positioned so that its lower edge was at a fixed height of 0.91 m (3 ft) above the floor to control direct sunlight and glare and admit daylight.

Simulations were performed for a clear sunny nine-day period in the summer and winter in two California climates, Oakland (moderate) and Burbank (moderate to hot). Hourly Typical Meteorological Weather (TMY) was used, where 5-min data was derived using a linear interpolation from hourly observations.

The Pacific Gas and Electric E-19 time-of-use rate schedule [PG&E, 2018] was used to reflect existing electricity rates in California ("TOU1"). This schedule has a monthly coincident peak demand charge based on the peak power consumption for different periods; i.e., for the highest priced summer period from noon to 6 PM, the maximum power consumption for this time period and over all days in the month sets the monthly demand charge of $19.65 per kW (summer). The other component of the E-19 tariff is a time-varying price for energy consumption, which is at its highest ($0.1606/kWh) during summer periods from noon to 6 PM. Finally, a monthly non-coincident demand charge of $17.74/kW is added for the highest 15 min of use regardless of when the peak occurs in the month. A second time-of-use rate schedule reflecting proposed updated PG&E commercial rates was also modeled ("TOU2") with time-varying prices for energy consumption and demand (E-19R, CALSEIA 2018). The non-coincident peak demand charge is $19.43 per kW and the energy price is $0.2152/kWh during summer peak periods from 5-10 PM. Note the shift in peak period from the afternoon to the late afternoon and evening hours. The two rates are summarized in Table 1. In order to preserve the ratio of monthly demand charge, which is based on the maximum peak over the whole month, and energy cost, which is based on the instant power consumption, weekly results for energy cost were extrapolated to four weeks, while the monthly demand charge was assumed to stay constant.

Table 1. TOU1 and TOU2 time-of-use electricity rate schedules.

		TOU1 (E-19)		TOU2 (E-19-R)
Time-of-use Energy Charge		($/kWh)		($/kWh)
Summer	Peak	$0.16055	Peak	$0.21517
	Partial Peak	$0.11613	Partial Peak	$0.14449
	Off-Peak	$0.08671	Off-Peak	$0.11158
Winter	Peak		Peak	$0.12935
	Partial Peak	$0.11004	Off-Peak	$0.11029
	Off-Peak	$0.09401	Super Off-Peak	$0.09384
Demand Charge		($ per kW)		($ per kW)
Summer	Max Peak	$19.65	Non-coincident	$19.43
	Partial Peak	$5.40	Peak summer	$0.48
	Maximum	$17.74		
Winter	Part Peak	$0.12		
	Maximum	$17.74		

	TOU1		TOU2	
Summer (May-Oct)	Peak	12:00 PM - 6:00 PM, weekdays (except holidays)	Peak	5:00 PM - 10:00 PM every day
	Partial Peak	8:30 AM - 12:00 PM, 6:00-9:30 PM, weekdays (except holidays)	Partial Peak	3:00-5:00 PM; 10:00 PM - 12:00 AM, every day
	Off-Peak	9:30 PM to 8:30 AM, weekdays (except holidays) and weekends	Off-Peak	All other hours
Winter (Nov-Apr)	Peak	None	Peak	5:00 - 10:00 PM, every day
	Partial Peak	8:30 AM to 9:30 PM, weekdays (except holidays)	Off-Peak	All other hours
	Off-Peak	9:30 PM to 8:30 AM, weekdays (except holidays) and weekends	Super Off-Peak	10:00 AM - 3:00 PM, March-May, all days of week

Four facade cases were modeled:

1) The “base” case is defined as the typical existing condition in commercial office buildings where the low-e window is shaded with a manually-operated, indoor fabric roller shade (Helioscreen gray, 3% openness factor) positioned at a fixed height of 0.91 m (3 ft) above the floor.
2) “Heuristic” is defined as a state-of-the-art, rule-based control algorithm, which was based on a prior field study of a commercially-available electrochromic window system in a large office building in Sacramento, California [Fernandes et al., 2017]. Each of the three EC window zones is progressively tinted so that the predicted transmitted illuminance is below a prescribed threshold. Threshold values are 4000, 8000, and 12,000 lux for the upper, middle, and lower control zones, respectively. The intent behind the algorithm is to control sky glare, preserve daylight, and minimize cooling loads due to solar heat gains.
3) “MPC1” control is defined by the model predictive control strategy described in Section 3.2. MPC1-d and MPC1-c denote discrete state and continuous tinting of the electrochromics, respectively. This case represents MPC control of the electrochromic window and lighting system to minimize TOU energy cost

due to HVAC and lighting over a 24-h prediction horizon, within glare, daylight quality and view constraints. The thermal comfort range (as defined by thermostat settings) was set to be the same as the heuristic case. In this scenario, the thermostat control was not integrated with the MPC controller, disabling any precooling capability.

4) "MPC2" is defined as the MPC1 case with precooling, where MPC control of the thermostat is enabled. MPC2-d and MPC2-c denote discrete state and continuous tinting of the electrochromics, respectively. Note that the air temperature is still maintained within the setpoint range for thermal comfort during occupied hours but because the setpoint range is broader during unoccupied hours, precooling could be implemented during early morning hours when energy costs are lower. For this case, the top surface of the concrete floor is exposed (carpet and pad were removed) in order to increase access to the floor slab thermal mass. While this action may slightly reduce peak HVAC demand alone, this case can be viewed as an integrated approach to enable and enhance load shifting through MPC control of HVAC, with the significant majority of any effect coming from the addition of MPC control of HVAC. For the emulator thermal model using the room heat balance model from the Buildings Library, the heat transfer between the air and the floor surface is modeled as natural convection on a horizontal flat surface where the heat transfer coefficient, h, is dependent on the temperature difference between the air and the floor, ΔT, and a coefficient, k:

$$h = k|\Delta T|^{0.3333} \text{ where } k = 0.76 \text{ if the air is warmer and } k = 1.51 \text{if the air is cooler.} \quad (6)$$

The parameters for the penalty functions in the MPC models were chosen based on a manual tuning process, conducted for selected days in the summer. For the DGPs penalty function, the parameters were gain, n, of 1, offset of 0, and an exponent of 6. The gain, n, for the derivative penalty was set to 10 and the gain of the view penalty, n, was set to 0. The parameters for the post-optimization were also chosen based on the same summer days. The summer parameters were used for the winter period.

4. Results

Results from the emulator simulations of heuristic and MPC control are given in the following figures and tables. Figures 8-9 show the performance of the heuristic controller and MPC1-d controller over a sunny summer period in Oakland with the TOU1 rate schedule. Zone warmup occurs over the first two days so data during this period should be ignored. Under heuristic control, all three EC zones tint progressively down to full tint in proportion to incident solar irradiation. Daylight illuminance is reduced at full tint, causing the electric lights to be turned on during mid-day hours, while solar heat gains are capped at about 100 W ($SHGC_{min}$=0.09). Discomfort glare is maintained below the DGP BIN (borderline between imperceptible and noticeable glare) of 0.34. Loads occur from both solar gains and the electric lighting, resulting in a total peak electric load in the late afternoon of 203 W. Under MPC1-d (d=discrete) control, the EC zones are not all fully tinted during mid-day such that the maximize daylight and view criteria are satisfied (1500-2000 lux), the electric lights are shut off, and discomfort glare is maintained below the DGP BND (borderline between noticeable and disturbing glare) of 0.38. Solar heat gains peak at 275 W, but the total electric load (with no lighting) peaks at 164 W. Monthly electricity cost with demand charges is $16.59 (heuristic) and $14.27 (MPC1-d), a savings of 14%. "Critical" peak demand (coincident demand) is reduced from 203 W to 164 W (19%). Note, savings are greater if the dynamic façade is able to provide continuous versus discrete state control. Monthly electricity cost is reduced by 23% and peak demand by 28% when using the MPC1-c (c=continuous) versus the heuristic controller. Overall, this example illustrates how the MPC1 controller is better able to weigh trade-offs between cooling and lighting energy use within constraints (glare) and qualitative requirements (daylighting and view) to provide a more optimal load shed response.

When comparing the performance of the MPC1-c and MPC2-c controllers (Figures 10-11), there are small differences between the two EC switching patterns that result in a flatter load shape with MPC2-c control of solar

heat gains. This complements the MPC2-c nighttime pre-cooling between midnight and early morning, allowing cooling to be shut off during the summer peak afternoon period. Glare, daylight and view criteria are met with both controllers. Monthly electricity cost is reduced from $12.81 to $11.91 (7%) and coincident peak demand is reduced significantly from 145 W to 117 W (20%) when MPC2-c is used instead of MPC1-c. These results illustrate how the combined control of building envelope loads with HVAC thermostat control can provide further load-modifying DR above and beyond that of envelope-only MPC control.

In this example, MPC2-c is intended to actively precool the space by thermally charging the concrete slab during the night, but is seen to be less effective due to model mismatch. At 8 AM when occupancy begins (Figure 11 "Temperatures"), the room air temperature sharply rises for the MPC1-c case, while the MPC2-c controller attempts to further charge the mass until around 10 AM. While the room air temperature for the MPC2-c case also sharply rises afterwards, the cooling power (Figure 11 "Electric Loads") is considerably lower than that of the MPC1 case from noon until 6 PM. The charged radiant slab provides cooling throughout the day and reduced peak load. To better explain the effect of model mismatch, Figure 12 shows an example of the projected room air temperature produced by the MPC2-c major optimization (colored lines for a 24 h prediction horizon for each 5 min interval). The dotted lines indicate the temperature band setpoints passed to the emulator. The black line shows the observed temperature from the emulator. The setpoints can be distinguished as floating (i.e., setpoint is at comfort range) or actively controlled (i.e., when precooling). It can be seen that until occupancy starts, the temperature tracks the projected temperatures. However, at 8 AM local time (x-axis "06-03 07" or 7 AM on the plot, in Standard Time) when occupancy starts, the room air temperature rapidly rises, whereas the earlier MPC2-c projections (blue lines) indicate coasting throughout the day without the need for mechanical cooling during the peak periods of the day. This is a strong indicator of overestimated thermal mass. Cost and demand savings indicated in the above paragraphs are therefore conservative.

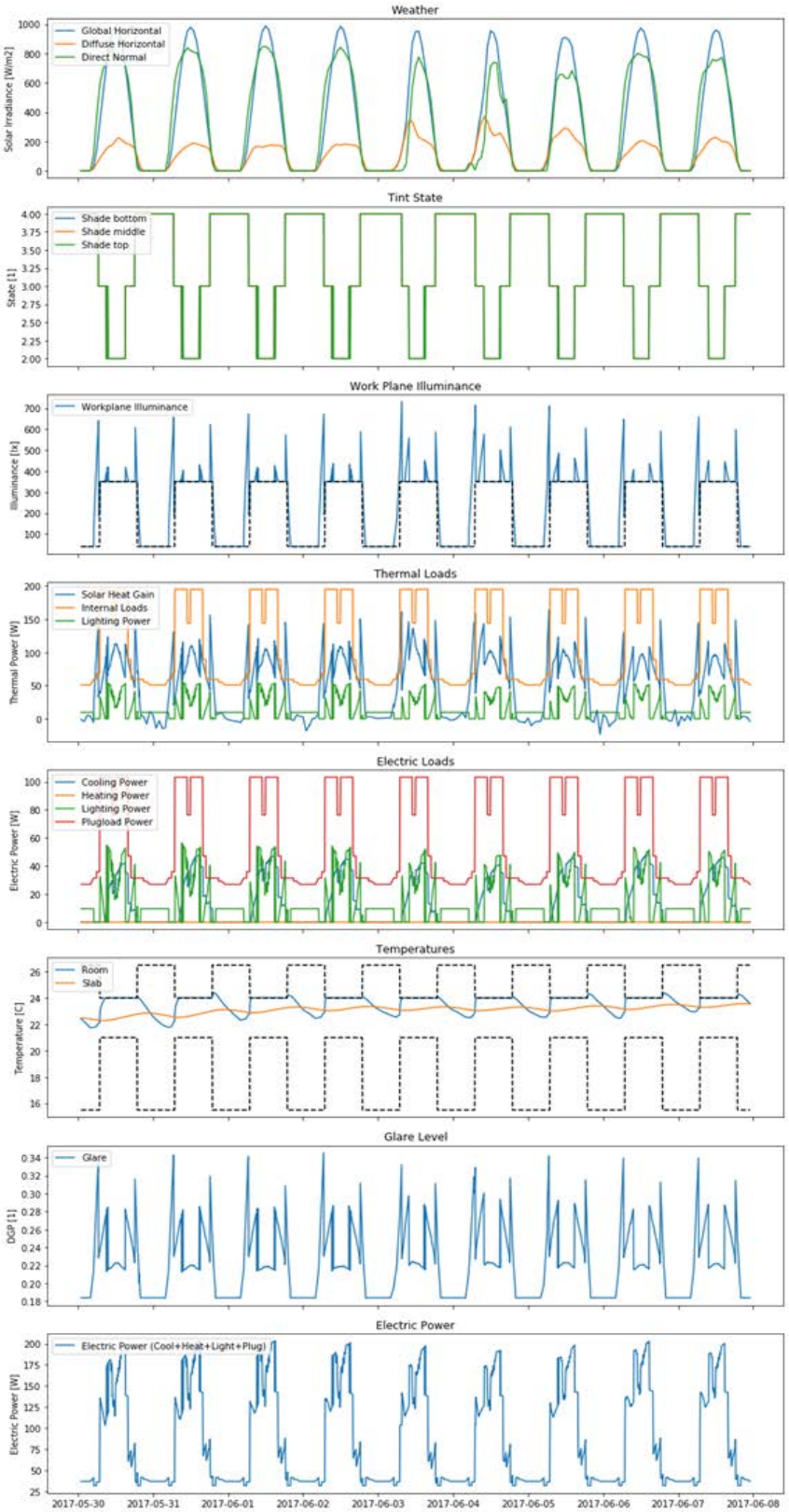

Graphs from top:
Outdoor solar irradiance (W/m^2);
Tint state of the three electrochromic zones (4 is clear, 1 is the darkest tint level);
Average room workplane illuminance from electric lights and daylight (350 lux setpoint dotted line);
Thermal loads from solar heat gains (does not include window conductive heat gains), internal loads from equipment and occupants, and electric lighting;
Cooling, heating, lighting, and plug load power use (including envelope conductive loads);
Room air and slab temperature (setpoint band shown with dotted line);
Daylight glare probability (DGP);
Total electric power use from cooling, lighting, and plug loads.
The first two days can be ignored.
Date label on the x-axis starts at midnight (Standard Time).
All data are from the emulator simulations (15-min average from 5-min modeled timestep).

Figure 8. Heuristic control over a nine-day sunny summer period, TOU1, Oakland.

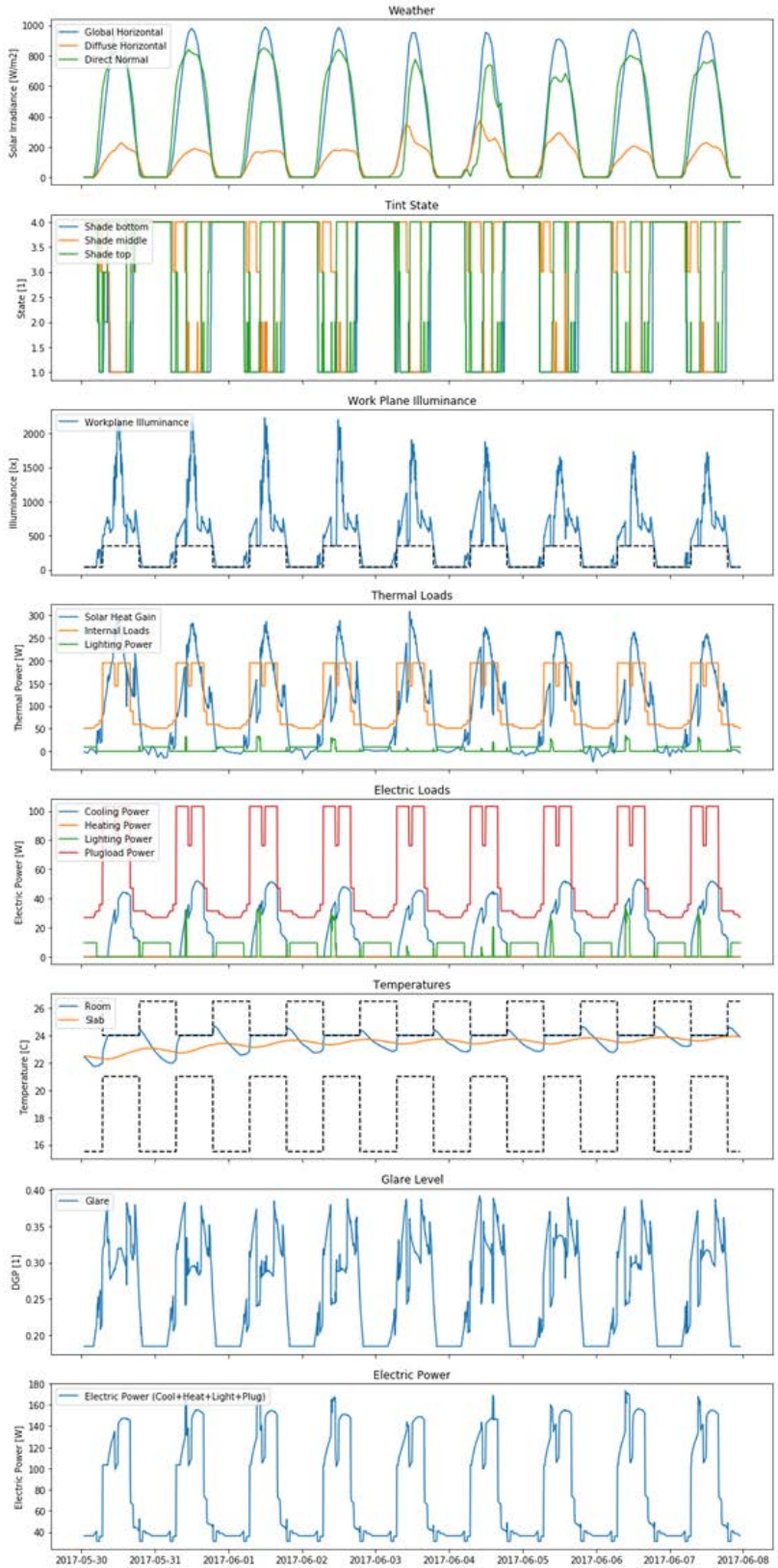

Figure 9. MPC1-d control over a nine-day sunny summer period, TOU1, Oakland.

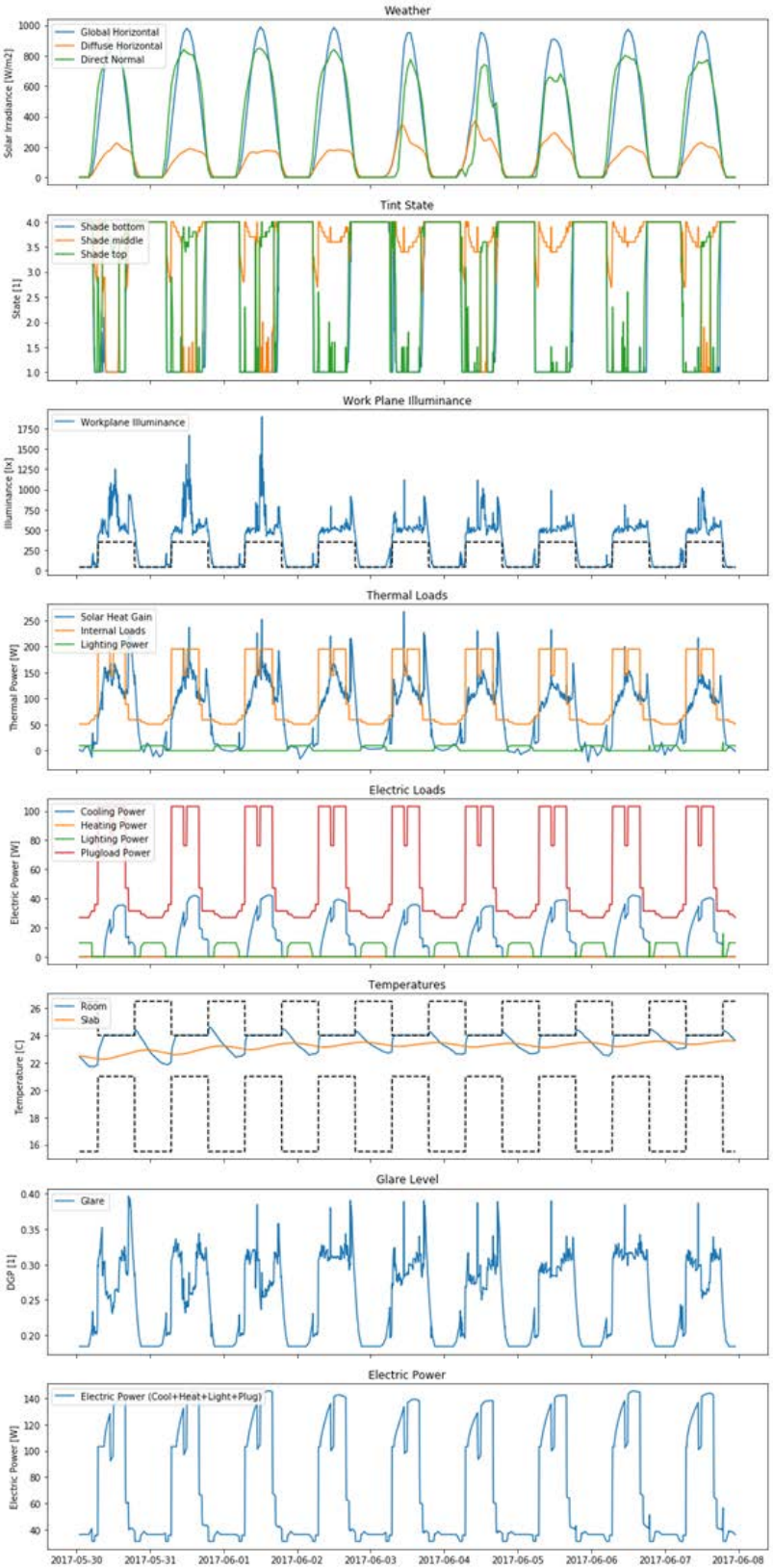

Figure 10. MPC1-c control over a nine-day sunny summer period, TOU1, Oakland.

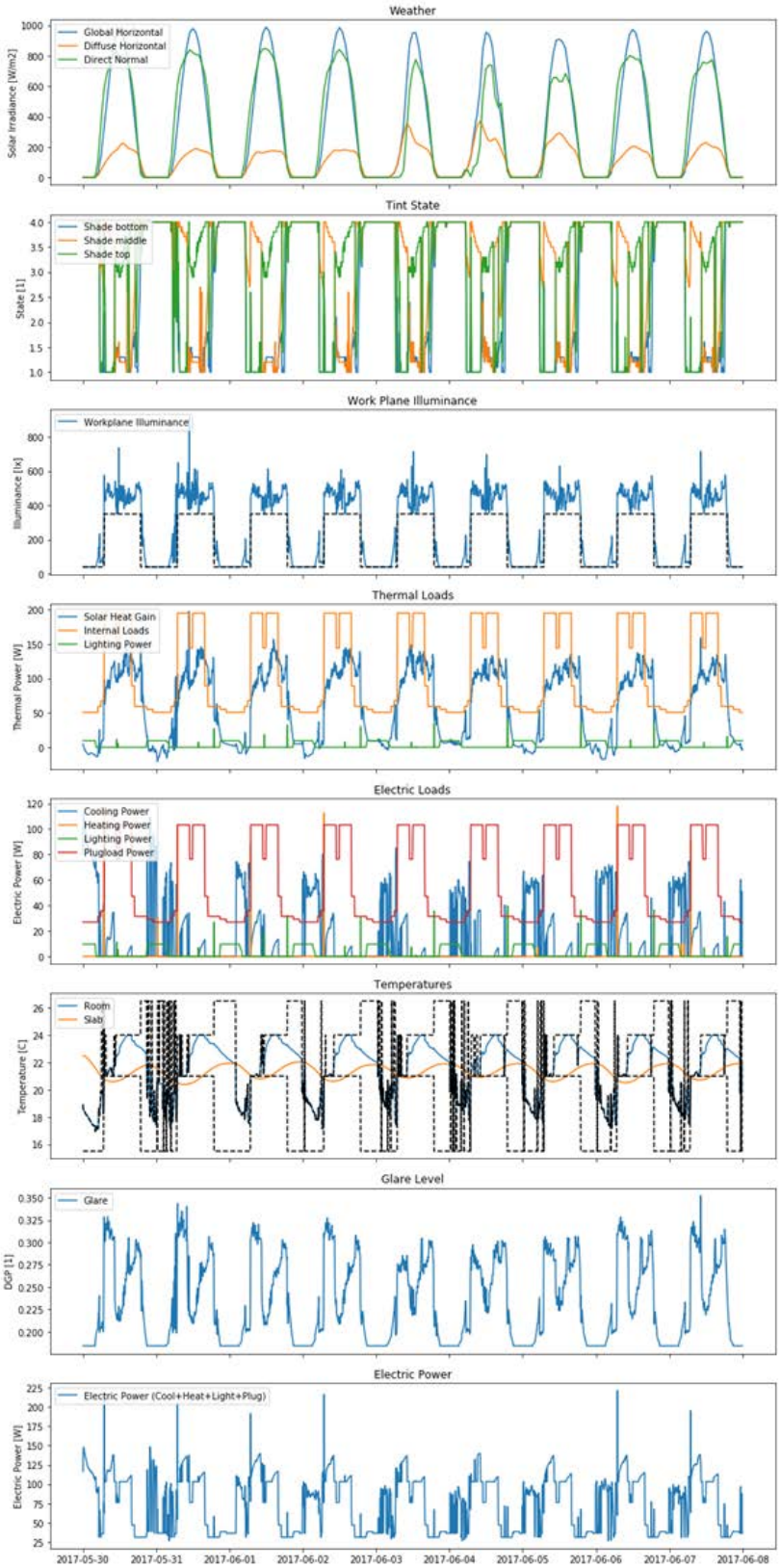

Figure 11. MPC2-c control over a nine-day sunny summer period, TOU1, Oakland.

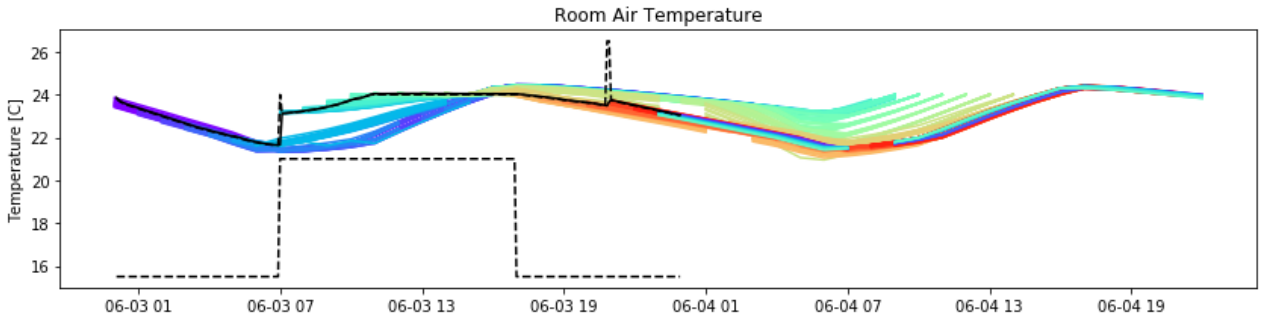

Figure 12. Example of projected room air temperature by the MPC2 major optimization and observed temperature from the emulator, in black. The colored lines show the projected MPC2 results for 24 h, for each 5-min control timestep, colored from violet in the morning to red in the evening.

The total electricity use profile for the five control modes can be seen in Figure 13, where the MPC schemes are shown to have provided significant load-modifying benefits during the summer period relative to the state-of-the-art reference case and heuristic controller. MPC1-d, MPC1-c, and MPC2-c were able to balance demands for both daylighting and solar heat gain control in proportion to energy and demand cost. With MPC2-c, the load shift from peak afternoon to off-peak nighttime periods provided by precooling in combination with daytime solar control is quite evident in this plot. Electric demand is nearly flat during the coincident peak period between noon and 6 PM (delineated by the dotted energy cost line). With the TOU2 rate schedule which shifts the coincident peak period towards evening hours (Figure 13b), the profiles however are almost identical. Small differences in load shape occur between MPC2-c with TOU1 versus TOU2 during the late afternoon hours just before 6 PM. This is due to the non-coincident (NC) peak demand charge (highest 15 min of use regardless of when it occurs) imposed by both rate structures, which strongly suppresses demand over the entire 24 h period.

There have been suggestions of eliminating NC demand charges so that incentives are more aligned with the wholesale electricity market requirements. Simulations were conducted to better understand how such changes would affect the load shape provided by MPC controls. If NC demand charges were eliminated, then the responsiveness of MPC control to coincident peak demand charges becomes much more apparent. This effect is illustrated for MPC2-c in Figure 14 (orange line). The morning peak of 225 W is due to morning cool down prior to occupancy; there is no pre-cooling at night to minimize peak loads in the morning period since there are only coincident demand charges for the 12-6 PM period. If demand charges are entirely eliminated (green line), there is minimal pre-cooling. During 12-6 PM period, peak demand is increased by 9% if there are no NC demand charges and by 22% if there are no demand charges at all (Table 2). This example demonstrates the flexibility of MPC to changes in utility rate structures that are likely to occur as California continues to adopt renewable energy.

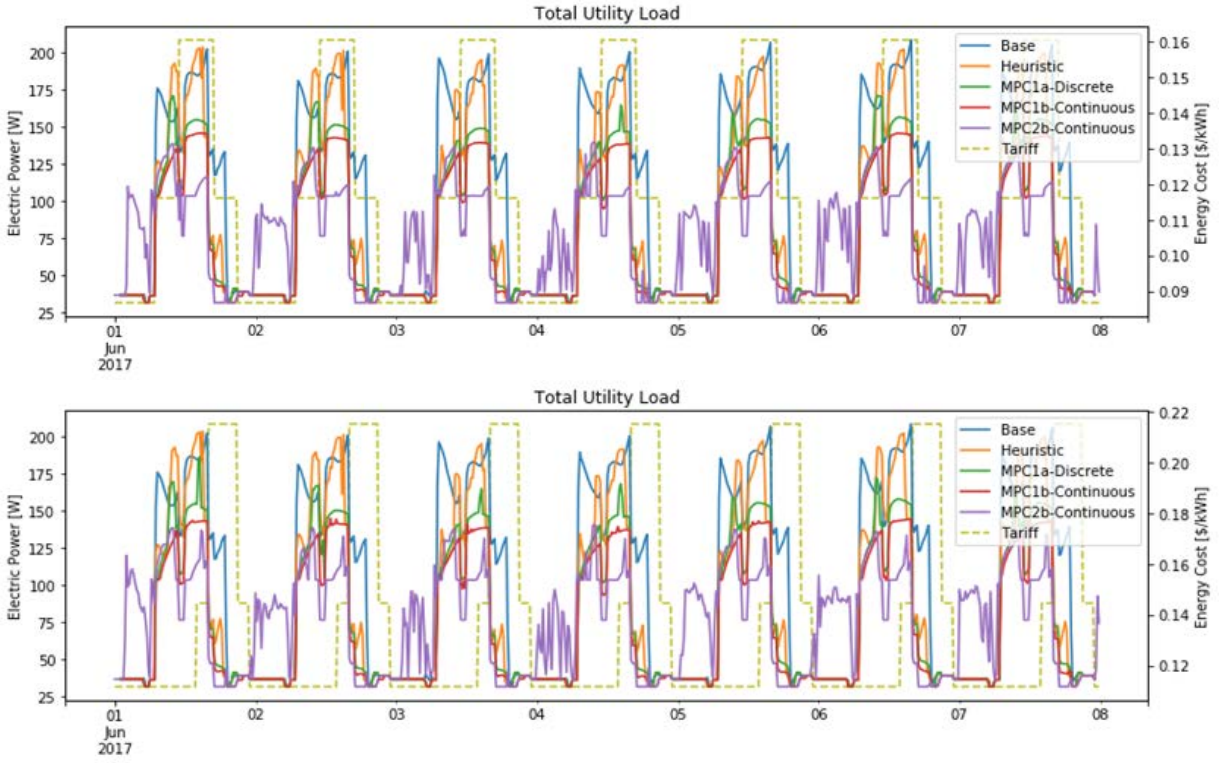

Figure 13. Total electricity demand versus time of day over a seven day sunny summer period for five control modes, Oakland for a) TOU1 (above) and b) TOU2 (below). Energy cost is shown as a dotted line on the graph.

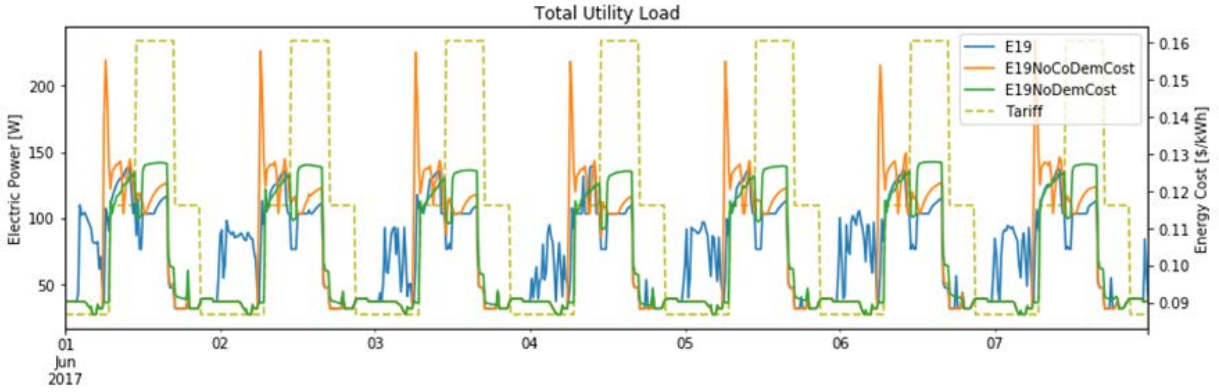

Figure 14. Total electricity demand versus time of day over a seven-day sunny summer period in Oakland. MPC2-c control is based on the TOU1 E-19 schedule, E-19 without non-coincident charges, and E-19 without any demand charges. Energy cost is shown as a dotted line on the graph.

Table 2. Monthly total energy cost ($) and peak demand (W) with and without coincident (C) and non-coincident (NC) demand charges for a south-facing perimeter zone with MPC2-c control and various TOU1 rate schedules during the summer, Oakland.

	Monthly cost ($)			Critical peak demand		
	Demand	Energy	Total	W	W/ft^2	(%)
E19	5.513	6.394	11.908	116.45	0.78	
E19, no NC demand charges	3.294	6.487	9.781	126.61	0.84	9%
E19, no NC or C demand charges		6.555	6.555	142.36	0.95	22%

Total monthly energy and demand cost, peak demand, and percent savings for the five original control strategies relative to the base case are given in Figures 15-16 and Table 3. Monthly data were derived from the seven-day modeled period. Compared to state-of-the-art heuristic control, MPC1 and MPC2 strategies reduced TOU1 total energy cost by 9-28% and coincident peak demand was reduced by up to 0.58 W/ft^2-floor or 19-43% on sunny summer days in Oakland. Similar savings were achieved for the hotter, Burbank climate in Southern California.

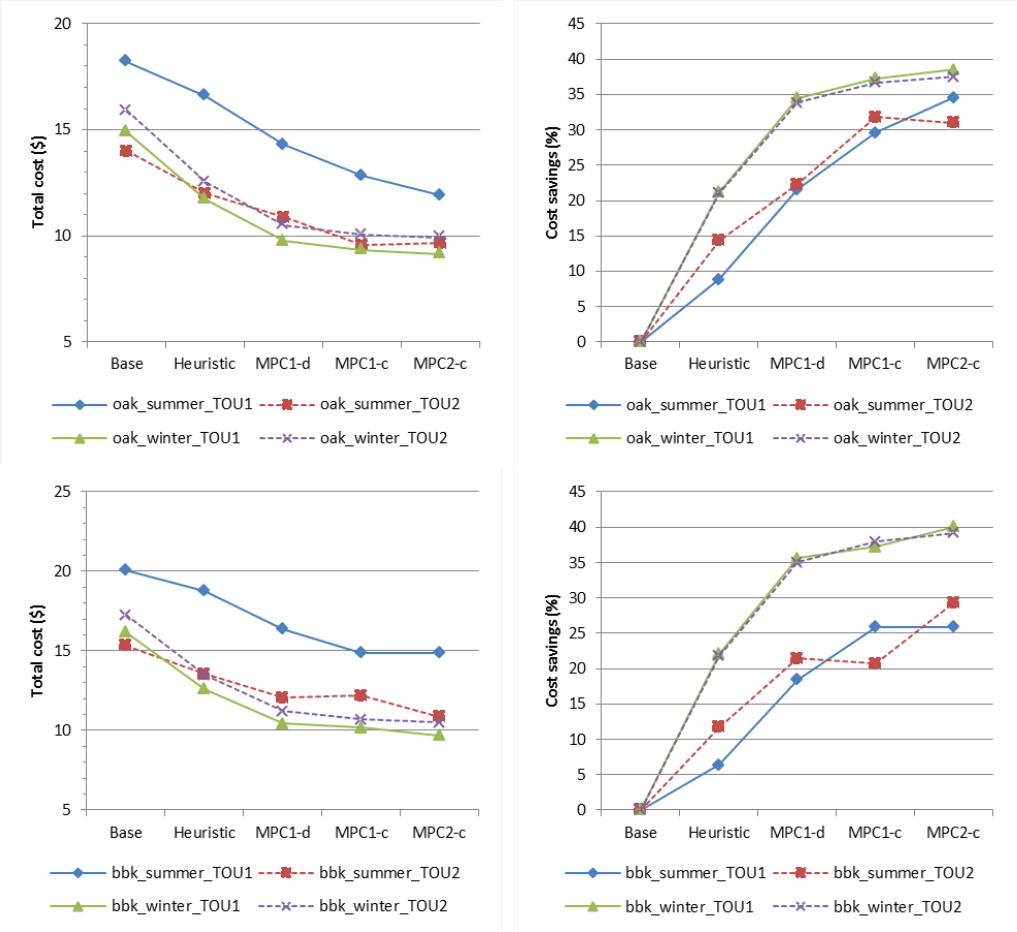

Figure 15. Total monthly electricity and demand cost (left) and percent savings (right) relative to the base case for a 13.9 m^2 (150 ft^2) south-facing perimeter zone in Oakland (above) or Burbank (below) given TOU1 or TOU2 utility rate schedules.

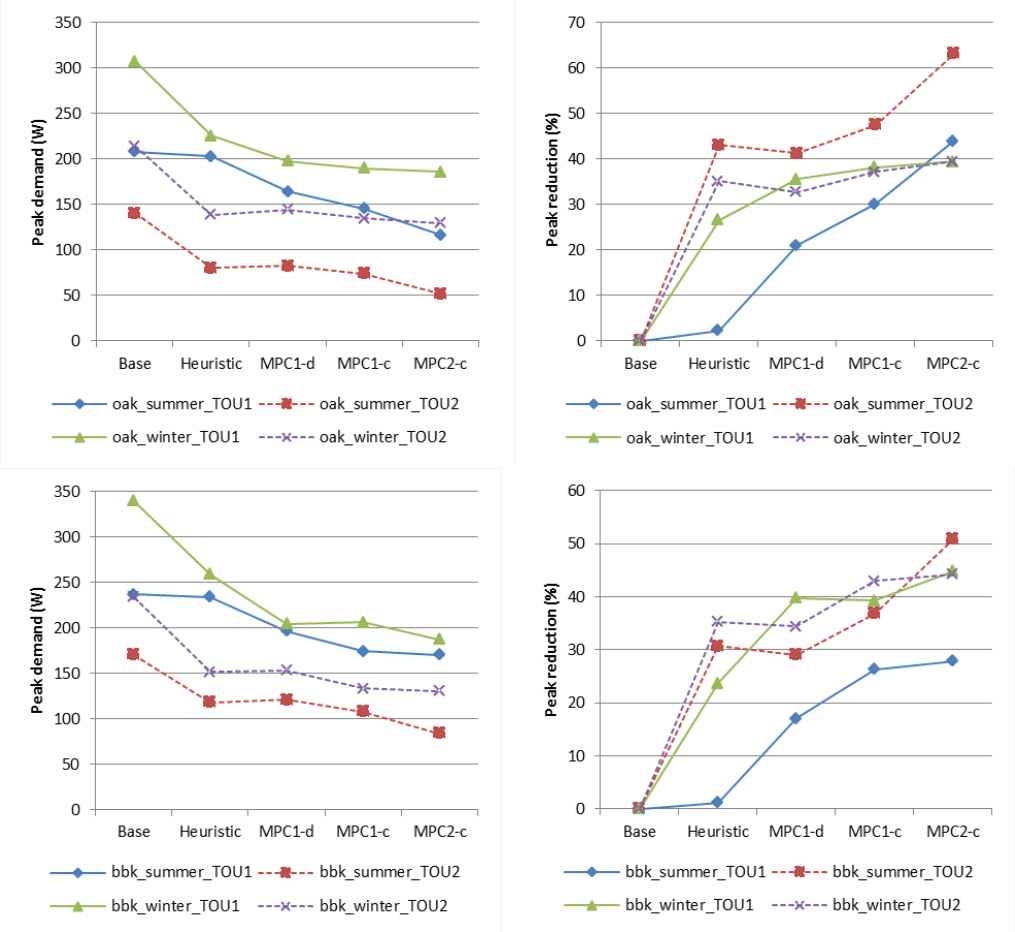

Figure 16. Critical coincident peak demand (left) and percent savings (right) relative to the base case for a 13.9 m^2 (150 ft^2) south-facing perimeter zone in Oakland (above) or Burbank (below) given TOU1 or TOU2 utility rate schedules.

Table 3. Total monthly energy and demand cost ($), coincident peak demand (W), and cost and demand savings (%) relative to the base case and heuristic controls.

Case	Oakland				Burbank			
	Summer		Winter		Summer		Winter	
	TOU1	TOU2	TOU1	TOU2	TOU1	TOU2	TOU1	TOU2
Monthly total energy cost ($)								
Base	18.202	14.004	14.887	15.881	20.063	15.348	16.181	17.240
Heuristic	16.592	11.991	11.731	12.532	18.789	13.546	12.612	13.480
MPC1-d	14.273	10.883	9.749	10.506	16.364	12.056	10.421	11.204
MPC1-c	12.814	9.555	9.333	10.057	14.868	12.174	10.158	10.694
MPC2-c	11.908	9.662	9.157	9.928	14.865	10.848	9.698	10.489
Cost savings relative to the base case (%)								
Heuristic	9%	14%	21%	21%	6%	12%	22%	22%
MPC1-d	22%	22%	35%	34%	18%	21%	36%	35%
MPC1-c	30%	32%	37%	37%	26%	21%	37%	38%
MPC2-c	35%	31%	38%	37%	26%	29%	40%	39%
Cost savings relative to heuristic control (%)								
MPC1-d	14%	9%	17%	16%	13%	11%	17%	17%
MPC1-c	23%	20%	20%	20%	21%	10%	19%	21%
MPC2-c	28%	19%	22%	21%	21%	20%	23%	22%
Critical peak demand (W)								
Base	208.18	140.47	307.33	214.35	237.05	170.90	339.68	234.24
Heuristic	203.27	80.00	225.56	139.05	234.33	118.34	259.27	151.62
MPC1-d	164.44	82.40	197.83	144.22	196.49	121.24	204.64	153.63
MPC1-c	145.44	73.74	189.88	134.74	174.63	107.87	206.34	133.54
MPC2-c	116.45	51.62	185.90	129.82	170.87	84.03	187.53	130.62
Peak demand savings relative to the base case (%)								
Heuristic	2%	43%	27%	35%	1%	31%	24%	35%
MPC1-d	21%	41%	36%	33%	17%	29%	40%	34%
MPC1-c	30%	48%	38%	37%	26%	37%	39%	43%
MPC2-c	44%	63%	40%	39%	28%	51%	45%	44%
Peak demand savings relative to heuristic control (%)								
MPC1-d	19%	-3%	12%	-4%	16%	-2%	21%	-1%
MPC1-c	28%	8%	16%	3%	25%	9%	20%	12%
MPC2-c	43%	35%	18%	7%	27%	29%	28%	14%

Monthly energy cost savings for the winter and summer periods were projected to a full year, assuming that the simulated sunny weeks were representative for each period.

- If the decision involves whether to use heuristic versus MPC controls (i.e., incremental cost of electrochromic windows is not included), then the projected annual energy cost savings between heuristic and MPC1-c is $\$0.51/ft^2$-window-yr. With an added cost for the MPC controller hardware of $39 per curtainwall unit ($\$0.54/ft^2$-window) [Gehbauer et al. 2018], the simple payback period is 1.1 years.
- If the decision involves whether or not to use autonomous MPC1 versus integrated MPC2 controls, then the projected annual energy cost savings between MPC1-c and MPC2-c is $\$0.09/ft^2$-window-yr with a simple

payback of 6 years, assuming the same incremental cost ($0.54/ft^2-window). Costs for enabling thermostat control and access to sensor data needed to tune the R2C2 network are assumed to be included as part of the base HVAC control system.

The computation time needed for the optimization is an important criterion for practical realization of real-time control in buildings. The control timestep was defined as 5 min, which is the time window for the optimization to complete. Figure 17 shows total control evaluation times for the different control strategies and seasons.

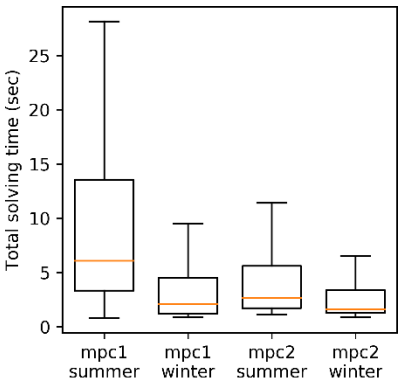

Figure 17. Total control solving times for strategy with (MPC2) and without (MPC1) integration with the HVAC system. Whiskers are defined at 25th and 75th percentile.

It can be seen that at any time, the solving times are well below the 5-min threshold, with a maximum at about 25 s. The summer season appears more challenging to solve, which can be attributed to the higher cost impact of electricity consumption, and the more complex three-stage TOU tariff, in comparison to the two-stage tariff in winter. The occupancy comfort may also contribute to the faster solving times, by a more restricted solution space due to low winter sun angles. The difference between the integration with HVAC, MPC2, and without integration, MPC1, are on average 4 s. It is to note that MPC1, on average, takes longer to compute than MPC2, which is non-intuitive, i.e., MPC2 with its integration with the HVAC system was expected being more complex to solve. However, in this development of the controller, the implementation of MPC1 was the same as MPC2, but MPC1 was constrained to allow very little temperature change approximating a constant setpoint. This method of constraining the controller was likely the root of the increased solving times for MPC1.

5. Discussion

5.1. Performance bound assumptions for the MPC simulation results

The introduced MPC optimization framework utilizes as much information as possible to provide optimal control. For this simulation study, inputs for forecasted weather, occupancy and internal loads were provided to the MPC controller. These inputs were the same as those passed to the emulator, assuming perfect knowledge of these quantities. As real-world deployment will show higher deviations, the presented MPC control performance is given as the best case scenario with respect to external disturbances.

On the other hand, the room model of the MPC controller was created solely from simple room and window dimensions which were entered through the user interface. The resistance-capacitance (RC) thermal model in the controller, which is typically parameterized through the user interface, represents a much simplified model of the Modelica model in the emulator and therefore represents, to some degree, the expected model mismatch in a field deployment. Overall, the results can be considered somewhere between a best case scenario and a well-tuned field

setup. Further analysis on the impact of uncertainties and model mismatch will need to be conducted to quantify impacts on the actual operations and energy cost.

Another simplification made was the exclusion of expected or previously set demand charges, which shifts the weight of the objective function towards peak demand reduction. While the results already show significant energy and peak demand savings, a future implementation including forecasted or previously set demand charge would rectify the relationship between peak demand and energy, to potentially further decrease cost.

5.2. Convexity of control optimization problem

Strictly speaking, the MPC problems solved in this study are non-convex, since the equality constraints defined by the model are nonlinear. The nonlinearity comes from the exponential functions [Gehbauer et. al., 2017] used to relate window tint level to daylighting, glare, and solar heat gain values (i.e., transmission levels decrease exponentially with tint states 1-4). Converting the problem to one that is convex would require linearization of this exponential relationship. Defining a single linear approximation significantly reduces the accuracy of the model, while defining a piecewise linear approximation changes the optimization problem to a nonlinear integer programming problem. With the current non-convex formulation, finding a global optimal is not guaranteed. However, the results of the simulations in this study empirically show the improved performance with the MPC controller over the heuristic. An exploration of alternative optimization problem formulations and their influence on the resulting control performance and computational requirements is planned for future work.

5.3. Model mismatch in the MPC controller

One key issue associated with the general field of model predictive controls is degradation in performance due to model mismatch. This term describes the difference in expected performance between that of the MPC controller and the actual simulated and real world, observed performance. Typically a measurement of error, i.e., root mean square error, is defined to evaluate the quality and accuracy of MPC models. However, for optimization purposes, the evaluation of individual component model performance is confounded since the models are used in combination with other models to determine the final control state. A model with moderate performance could lead to the same or very close performance as a perfect model, if the model's performance metric is defined as the objective of the optimization. One reason is the compensation of errors by the aggregation of the component models in the objective function, where one model error could compensate for another model's error. Another reason why accuracy limits of component models are hard to determine is the re-iteration through the optimization, when formulated as MPC. One example could be a reduced order thermal model in the form of an R2C2 network. If projected for one hour, the model performance might be moderate to poor. But if the state of the model is periodically updated the current room temperature, e.g., at each 1- or 5-min timestep, then the performance might be significantly better.

For the introduced Dynamic Facade Control agent, the objective of minimizing total energy cost using TOU rates was defined, where the controller must lower or shift thermal loads to avoid expensive peak demand charges. Accurate projections over several hours are therefore necessary, which then defines the requirements for the model. The final model performance must therefore be evaluated based on the defined objective. As indicated above, the evaluation gets even more complex with multiple sub- or component models. For illuminance and glare, the Radiance three-phase method was used for both the MPC controller and the emulator. However, the emulator geometric model was more detailed than that used for the MPC controller, surface reflectance data were matched to that of the full-scale LBNL Advanced Windows Testbed facility, and finally models were fit to polynomial tint functions to feed the MPC model. All of these differences resulted in differences in predicted and actual performance. The primary source of discrepancies between the MPC controller and emulator were the models used to predict solar heat gain and room thermal response. To improve the thermal response model, a continuous tuning

process was implemented where the R and C parameters are periodically tuned, i.e., every hour, based on the latest data recorded from the building. Further work is needed however to improve controller accuracy.

5.4. Suitability of the modeling framework

The introduced tool-chain of JModelica.org and MPCPy is a convenient and straightforward method to design or parameterize a Modelica model and then optimize the model for a defined objective. Each execution of the tool-chain, with the predefined model, takes environmental conditions and other optional user inputs, to compute an optimal solution. This solution can be described as static, where changing environmental conditions, internal conditions, or supervisory operation are not taken into account. In order to allow for dynamic adaptation, the static optimization can be re-evaluated with updated inputs. This dynamic adaptation is typically referred to as model predictive control. However, the remaining challenge is the actual implementation as a building controller, with the open questions of implementation of optimal setpoints, integration of occupant feedback, resilience against internal or external disturbances, and finally the necessary effort for system integration.

The level of abstraction in the introduced tool-chain might benefit the building designer to parameterize predefined models, but complicates the development of models. One issue is the lack of support for binary variables to implement conditional control statements. JModelica.org currently only supports three solvers, the open-source Interior Point OPTimizer (IPOPT), proprietary We Optimize Really Huge Problems (WORHP) algorithm, and an implementation of the Nelder-Mead algorithm. IPOPT and WORHP are both large-scale nonlinear solvers, which do not support integer or binary implementations, while the Nelder-Mead algorithm is a derivative-free numeric algorithm that is inefficient for control optimization problems [Wetter et al. 2016]. In other optimization languages, such as General Algebraic Modeling System (GAMS) or the Python-based Pyomo, solvers are freely chosen based on the problem defined. This is considerably more flexible, but on the other hand requires the user to manually enter the system of equations and constraints to be solved. If binary variables are necessary, users can typically choose between two options: mixed-integer linear programming (MILP) and mixed-integer nonlinear programming (MINLP). While it is possible to approximate nonlinear models as linear systems, to benefit from the efficiency boost of solving linear system, this work focuses on nonlinear models. The only option to utilize binaries in such an environment would be a MINLP implementation. This conversion would solve several issues with the current implementation, where for example tint states are discrete quantities, but are reflected as continuous signal within the NLP implementation. This requires an additional step of heuristic selection in the conversion, which leads to suboptimal control of the assets. Another issue which was noted in the development of the framework is the difficult debugging due to the many layers of abstraction. While optimization problem equations are implemented directly in other tools, JModelica.org requires a system of differential-algebraic equations (DAE) be implemented in Modelica. The DAE system is then discretized in time and transformed to optimization problem equations, redefined in a format readable by the solver. Additional abstraction added by the MPCPy framework can make error debugging or the simple tracing of signals significantly more difficult than in other optimization tools. Finally, the solver IPOPT exploits the first and second derivatives, which requires the objective and constraints to be twice continuously differentiable. In addition, while the solver can provide local solutions only, it will provide global solutions for convex problems. It is therefore desirable to formulate the optimization problem as convex. The levels of abstraction provided by Modelica libraries in model implementation and JModelica.org in generating optimization problems from Modelica models can make it difficult to analyze the final structure of the internally generated optimization problem. This turned out problematic when developing new model structures or during debugging, because of the lack of insight into the actual optimization problem which is finally solved by IPOPT.

The tradeoff between the complexity of the optimization problem and time resolution of the control signal to be implemented requires a definition of the maximal allowable time per iteration. This is equal to the real-time criteria, or smallest time step necessary to fulfill the control operation. The initial design focused on user comfort, such as glare and daylighting where time constants are typically slow, with reaction times on the order of minutes. The

controller was therefore designed to meet the criteria, with a design timestep of 5 min. However, the further advancement of the controller to incorporate thermal load management and consideration of TOU prices, decreased the reaction time to less than a minute. The current computation takes around 20 s per timestep to meet this stringent requirement. However, this timing test is performed using a standard desktop computer with significantly more computing power than the target platform which is an embedded controller. Further tests with the deployed controller on the target platform will have to be conducted, to ensure the real-time criteria are met. In addition, the criteria itself would have to be redefined to ensure highest comfort and lowest energy cost at any level of disturbance.

6. Conclusions

A simulation study was conducted to evaluate the load modifying potential of dynamic facades in support of California's overarching goal to reduce greenhouse gas emissions by 40% below 1990 levels by 2030. The study evaluated two prototype model predictive controllers, one with precooling, the other without, using an emulator to evaluate resultant perimeter zone energy demand. The emulator was based on validated models from the Modelica Buildings Library and the Radiance three phase matrix algebraic method. Energy use costs resulting from the MPC controllers were compared to that of state-of-the-art heuristic control of a three-zone electrochromic window (SHGC=0.09-0.41, Tvis=0.01-0.60) in a south-facing perimeter office zone in Oakland and Burbank, California. Two time-of-use utility rate structure were used in the analysis: the TOU1 coincident peak summer period was 12-6 PM while the TOU2 period was 5-10 PM.

The MPC1 controller was designed to minimize total energy and demand costs through control of the electrochromic window and dimmable lighting system. MPC1 reduced total perimeter zone energy costs by 13-23% (TOU1) and 9-20% (TOU2) compared to heuristic control on clear summer days in Oakland and Burbank. Energy costs were reduced by similar percentage savings on sunny winter days. Critical peak demand was reduced by 0.26-0.39 W/ft^2-floor (19-28%) in the 15-ft deep perimeter zone during the 12-6 PM summer period (TOU1) compared to heuristic controls. Continuous tint control of the electrochromic yielded significantly greater savings compared to discrete (stepped) tint control.

The MPC2 controller was designed to minimize total energy and demand costs through control of the window, lighting, and HVAC thermostat, assuming that the top surface of the concrete floor slab was uncarpeted and directly exposed to the room air. Energy cost savings during sunny summer conditions were 21-28% (TOU1) and 19-20% (TOU2) compared to heuristic control. Critical peak demand was reduced by 0.42-0.58 W/ft^2-floor (27-43%) in the 15-ft deep perimeter zone during the 12-6 PM summer period (TOU1) in Oakland and Burbank compared to heuristic controls. Winter savings were similar. If the non-coincident peak demand charges are removed from the utility rate structure, then the MPC2 controller was demonstrated to adapt to the TOU1 and TOU2 coincident demand charges. This example provided evidence of the substantial power of MPC controllers to generate load shape and shift capabilities under an evolving electricity market.

Daylight requirements and glare constraints were met with both the MPC1 and MPC2 controllers. The heuristic controller resulted in significantly lower daylight illuminance (<350 lux) and therefore poorer daylight quality in the space. The MPC controllers provided both discomfort glare control, useful daylight (350-2000 lux), and view, both constraints of which can be tuned by the end user throughout the life of the installation. Solar heat gains were also controlled to minimize HVAC loads. Passive solar heating strategies and thermal comfort were not investigated in this study but their inclusion in MPC control could further reduce GHG emissions by offsetting the need for natural gas.

The MPC controller proved to be a very complex optimization problem because of the breadth of the parameters included in the optimization and the number of potential solutions given the three zone electrochromic, four discrete

tint states, dimmable lighting and thermostat control over a 24-h prediction horizon, and fast control time step needed for glare control. This project addressed many challenges regarding runtime, convergence, and infeasibility. Solving these challenges was hindered in part by the high level of model abstraction that occurred when Modelica models were automatically converted to an optimization problem by a variety of third-party tools. The optimization problem was divided into major and minor optimization processes to reduce runtime and complexity of the optimization model to be solved. Several options were investigated to improve the likelihood of finding an optimum and reduce the possibility of infeasible outcomes. A simulation model was used to determine the initial guess of the control solution prior to optimization but was found to require more runtime compared to optimizations without the provision. A static initialization of the optimization solver IPOPT was provided instead. Because a gradient-based, non-linear optimization solver was used, conversion from discrete control states to continuous control for optimization then back to discrete control was necessary. This conversion resulted in less than optimal results. Model mismatch will occur between the MPC controller and real-world conditions and a solution for automated tuning of model parameters was implemented. Likely sources of model discrepancies were identified and model improvements were suggested for future work.

A considerable amount of effort was expended to develop, debug, and test new models for use in the emulator. The Radiance three-phase method was implemented and the resultant solar radiation on room and window layer surfaces was integrated within the facade and room thermal heat balance calculations (building on an initial implementation made by [Noudui et al. 2012]). New methods were developed for optimizing control with time-of-use energy and demand rate schedules. Further work is needed to quantify the benefits of integrated dynamic facade control with precooling given an improved thermal network model and greater access to thermal energy storage by the HVAC system. Considerable work is needed to develop robust, reliable and cost-effective commercial MPC solutions. The prototype technology described in this study will be further developed to address the challenges of scaling up to the real-world context.

Based on this study, we conclude that there can be significant benefits from using model predictive controls above and beyond that of state-of-the-art dynamic facade controls. The magnitude of energy cost and peak demand reductions however are strongly dependent on the specific application, how the utility rates are structured, and how rates will evolve over the life of the installation. Given uncertainty in the electricity markets, the decision by industry to invest in MPC controls for dynamic facades and its valuation in the market will most likely not be based solely on whether its levelized cost is competitive against other DR resources. It will more likely be based on a complex mix of arguments that include energy efficiency, load-modifying DR, projected site energy cost savings, capital cost reductions, possible improved comfort, health, and indoor environmental quality, increased user amenity and satisfaction, and improved facility operations, all of which lead to greater market competitiveness in the real estate market.

Acknowledgments

This work was supported by the California Energy Commission through its Electric Program Investment Charge (EPIC) Program on behalf of the citizens of California and the Assistant Secretary for Energy Efficiency and Renewable Energy, Building Technologies Program, of the U.S. Department of Energy, under Contract No. DE-AC02-05CH11231.

The authors would like to thank Dustin Davis at the California Energy Commission and Marc LaFrance and Amir Roth at the U.S. Department of Energy for their continued support for this research. We would like to also acknowledge our LBNL colleagues Thierry Nouidui and Daniel Fuller for their technical support for this research.

References

Åkesson, J., Gäfvert, M., and Tummescheit, H., 2009. JModelica—an Open Source Platform for Optimization of Modelica Models. In 6th Vienna International Conference on Mathematical Modelling, February 11-13, 2009.

Alstone, P., Potter, J., Piette, M.A., Schwartz, P., Berger, M.A., Dunn, L.N., Smith, S.J., Sohn, M.D., Aghajanzadeh, A., Stensson, S. and Szinai, J., 2017. 2025 California Demand Response Potential Study-Charting California's Demand Response Future: Final Report on Phase 2 Results. LBNL-2001113, Lawrence Berkeley National Laboratory, Berkeley, CA.

Andersson, J., Akesson, J., Diehl, M., 2012. CasADi: A Symbolic Package for Automatic Differentiation and Optimal Control. Recent Advances in Algorithmic Differentiation (87): 297-307.

Blum, D.H., Wetter, M., 2017. MPCPy: An Open-Source Software Platform for Model Predictive Control in Buildings. Proceedings of the 15th Conference of International Building Performance Simulation (IBPSA), San Francisco, CA, Aug 7 – 9, 1694-1703.

Blum, D., Jorissen, F., Huang, S., Chen, Y., Arroyo, J., Benne, K., Li, Y., Gavan, V., Rivalin, L., Helsen, L., Vrabie, D., Wetter, M., Sofos, M. 2019. Prototyping the BOPTEST framework for simulation-based testing of advanced control strategies in buildings. Accepted for publication in the Proceedings of IBPSA Building Simulation 2019. Rome, Italy, Sep 2-4.

California ISO (CAISO), 2016. What the duck curve tells us about managing a green grid, California ISO Fast Facts, Folsom CA. https://www.caiso.com/Documents/FlexibleResourcesHelpRenewables_FastFacts.pdf, accessed September 15, 2018.

California Energy Commission (CEC), 2015. 2016 Building Energy Efficiency Standards for Residential and Nonresidential Buildings. Publication Number: CEC-400-2015-037-CMF, June 2015.

California Energy Commission (CEC), 2017. The Electric Program Investment Charge: Proposed 2018 – 2020 Triennial Investment Plan. Publication Number: CEC-500-2017-023-CMF.

CALSEIA 2018. Proposed TOU Periods and Illustrative Rates. California Solar Energy Industries Association (CALSEIA). Accessed April 22, 2019: https://static1.squarespace.com/static/54c1a3f9e4b04884b35cfef6/t/5898f209d2b857d7c2d7685b/1486418442805/IOU+proposed+TOU+periods+and+rates.pdf

Coffey, B., 2012. Integrated control of operable fenestration systems and thermally massive HVAC systems: Methods and simulation studies of energy savings potential. Lawrence Berkeley National Laboratory, Berkeley, CA. http://eta-publications.lbl.gov/sites/default/files/mpc-shading-thermal-mass.pdf, accessed September 15, 2018.

Cutsem, O.V., Blum, D., Kayal, M., and Pritoni, M. 2019. Comparison of MPC Formulations for Building Control under Commercial Time-of-Use Tariffs. Proceedings of the 13th IEEE PES PowerTech. Milan, Italy, Jun 23-27. Accepted.

De Coninck, R. and Helsen, l., 2016. Practical implementation and evaluation of model predictive control for an office building in Brussels, Energy and Buildings (111): 290-298.

Deru, M., Field, K., Studer, D., Benne, K., Griffith, B., Torcellini, P., Liu, B., Halverson, M., Winiarski, D., Rosenberg, M. and Yazdanian, M., 2011. US Department of Energy commercial reference building models of the national building stock. https://www.nrel.gov/docs/fy11osti/46861.pdf, accessed September 15, 2018.

Fernandes, L.F, Lee, E.S., Dickerhoff, D., Thanachareonkit, A., Wang, T., Gehbauer, C., 2017. Electrochromic Window Demonstration at the John E. Moss Federal Building, 650 Capitol Mall, Sacramento, California. General Services Administration, Green Proving Ground Report, November 2016.

Functional Mockup Interface (FMI), https://fmi-standard.org/, accessed September 15, 2018.

Gehbauer, C., Blum, D.H., Lee, E.S., 2017. Integrated Dynamic Facade Control with an Agent-based Architecture for Commercial Buildings. Technical deliverable "High-Performance Integrated Window and Façade Solutions for California", California Energy Commission EPC-14-066, Task 6, July 14, 2017.

Gehbauer, C., Blum, D.H., Lee, E.S., Prototype Engineered Curtain Wall Unit. Technical deliverable "High-Performance Integrated Window and Façade Solutions for California", California Energy Commission EPC-14-066, Task 6, January 16, 2018.

Genopt, https://simulationresearch.lbl.gov/GO/, accessed September 15, 2018.

Gyalistras, D. and Gwerder, M. (Eds.), 2010. Use of weather and occupancy forecasts for optimal building climate control (OptiControl): Two years progress report. Terrestrial Systems Ecology ETH Zurich, Switzerland and Building Technologies Division, Siemens Switzerland Ltd., Zug, Switzerland, 158 pp, Appendices, ISBN 978-3-909386-37-6.

HSL 2019, a collection of Fortran codes for large-scale scientific computation. URL <http://www.hsl.rl.ac.uk/>

IBPSA, https://ibpsa.github.io/project1/, accessed September 15, 2018.

IPOPT, https://projects.coin-or.org/Ipopt, accessed September 15, 2018.

McNeil, A., Lee, E.S., 2013. A validation of the Radiance three-phase simulation method for modelling annual daylight performance of optically complex fenestration systems. Journal of Building Performance Simulation 6(1): 24–37.

Modelica, https://www.modelica.org/, accessed September 15, 2018.

Modelica Association, 2013. Modelica libraries. https://www.modelica.org/libraries, accessed September 15, 2018.

Nouidui, T.S., Wetter, M., Zuo, W., 2012a. Validation of the window model of the Modelica Buildings library. In Proc. of the 5th SimBuild Conference, Madison, WI.

Nouidui, T. S., K. Phalak, W. Zuo, and M. Wetter. 2012b. "Validation and Application of the Room Model of the Modelica Buildings Library." In Proceedings of the 9th International Modelica Conference. Munich, Germany, September. Modelica Association.

PG&E 2018. Pacific Gas & Electric (PG&E), Electric Schedule E-19 Medium General Demand-Metered TOU Service, effective May 10, 2010; accessed September 15, 2018: https://www.pge.com/tariffs/tm2/pdf/ELEC_SCHEDS_E-19.pdf.

PyFMI, https://github.com/modelon/PyFMI, accessed September 15, 2018.

Radiance, https://www.radiance-online.org/, accessed September 15, 2018.

Sällberg, E., Lind, A., Velut, S., Åkesson, J., Yances, S., Link, K., 2012. Start-up Optimization of a Combined Cycle Power Plant. 9th International Modelica Conference, Munich, Germany.

SOEP, Spawn of EnergyPlus, DOE-BTO, 2018. https://www.energy.gov/eere/buildings/downloads/spawn-energyplus-soep, accessed September 15, 2018.

Sturzenegger, D., Gyalistras, D., Morari, M., Smith, R.S., 2016. Model Predictive Climate Control of a Swiss Office Building: Implementation, Results, and Cost–Benefit Analysis, IEEE Transactions on Control Systems Technology 24 (1), 2016.

Wachter, A., Biegler, L.T., 2006. On the implementation of an interior-point filter line-search algorithm for large scale nonlinear programming. Mathematical Programming (106): 25-57.

Wei, M., Nelson, J.H., Greenblatt, J.B., Mileva, A., Johnston, J., Ting, M.K., Yang, C., Jones, C.M., McMahon, J.E., Kammen, D.M., 2013a. Deep carbon reductions in California require electrification and integration across economic sectors. Environmental Research Letters 8 (2013) 014038.

Wei, M., Nelson, J.H., Greenblatt, J.B., Mileva, A., Johnston, J., Ting, M.K., Yang, C., Jones, C.M., McMahon, J.E., Kammen, D.M., 2013b. Supplementary Material for Deep carbon reductions in California require electrification and integration across economic sectors. Environmental Research Letters 8.1.

Wetter, M., Zuo, W., Nouidui, T. S., Pang, X., 2014. Modelica buildings library. Journal of Building Performance Simulation 7(4): 253–70.

Wetter, M., Bonvini, M., and Nouidui, T.S. 2016. Equation-based languages - A new paradigm for building energy modeling, simulation and optimization. Energy and Buildings, 117:290–300, 2016.

Wienold, J., 2009. Dynamic daylight glare evaluation. In Eleventh International IBPSA Conference: Building Simulation. www.ibpsa.org/proceedings/BS2009/BS09_0944_951.pdf, accessed September 15, 2018.

WINDOW, https://windows.lbl.gov/software/window, accessed September 15, 2018.